LOW FREQUENCY GEOMAGNETIC FLUCTUATIONS (.01 TO 3 Hz) ON THE FLOOR OF MONTEREY BAY

Edmund J. Chaffee

NAVAL POSTGRADUATE SCHOOL
Monterey, California

THESIS

LOW FREQUENCY
GEOMAGNETIC FLUCTUATIONS (.01 TO 3 Hz)
ON THE FLOOR OF MONTEREY BAY

by

Edmund J. Chaffee

December 1979

Thesis Advisor: O. Heinz

SECURITY CLASSIFICATION OF THIS PAGE (When Data Entered)

REPORT DOCUMENTATION PAGE

READ INSTRUCTIONS BEFORE COMPLETING FORM

1. REPORT NUMBER	2. GOVT ACCESSION NO. / 3. RECIPIENT'S CATALOG NUMBER
4. TITLE (and Subtitle): Low Frequency Geomagnetic Fluctuations (.01 to 3 Hz) on the Floor of Monterey Bay	5. TYPE OF REPORT & PERIOD COVERED: Masters Thesis; December 1979. / 6. PERFORMING ORG. REPORT NUMBER
7. AUTHOR(s): Edmund J. Chaffee	8. CONTRACT OR GRANT NUMBER(s)
9. PERFORMING ORGANIZATION NAME AND ADDRESS: Naval Postgraduate School, Monterey, California 93940	10. PROGRAM ELEMENT, PROJECT, TASK AREA & WORK UNIT NUMBERS
11. CONTROLLING OFFICE NAME AND ADDRESS: Naval Postgraduate School, Monterey, California 93940	12. REPORT DATE: December 1979 / 13. NUMBER OF PAGES: 90
14. MONITORING AGENCY NAME & ADDRESS (if different from Controlling Office): Naval Postgraduate School, Monterey, California 93940	15. SECURITY CLASS. (of this report): Unclassified / 15a. DECLASSIFICATION/DOWNGRADING SCHEDULE

16. DISTRIBUTION STATEMENT (of this Report)

Approved for public release; distribution unlimited.

17. DISTRIBUTION STATEMENT (of the abstract entered in Block 20, if different from Report)

18. SUPPLEMENTARY NOTES

19. KEY WORDS (Continue on reverse side if necessary and identify by block number)

Low frequency geomagnetic measurements
Geomagnetic fluctuations in an ocean environment

20. ABSTRACT (Continue on reverse side if necessary and identify by block number)

Using a Cs vapor magnetometer, fluctuations of the total magnetic field in the .01 Hz to 3 Hz frequency range were observed on the floor of Monterey Bay, California. Fourteen hours of data were recorded over a period of six months in 1979 at several depths from 30 to 300 meters. A small, inexpensive recording system was designed and manufactured having a noise floor below 10^{-3} nT in the frequency range of

DD FORM 1 JAN 73 1473 EDITION OF 1 NOV 65 IS OBSOLETE
S/N 0102-014-6601 |
(Page 1)

SECURITY CLASSIFICATION OF THIS PAGE (When Data Entered)

interest. Data analysis includes an ocean wave/geomagnetic fluctuation comparison along with a qualitative analysis of the power spectra of the fourteen hours of geomagnetic fluctuation data. Typical geomagnetic fluctuation spectrum levels were found to be about 1 $(nT)^2/Hz$ at .01 Hz. As the frequency increased, the magnitude of the spectrum decreased to approximately 10^{-5} $(nT)^2/Hz$ at 3 Hz. Correlation between ocean wave period and peaks in the geomagnetic fluctuation spectra was observed.

Approved for public release; distribution unlimited

Low Frequency Geomagnetic Fluctuations (.01 to 3 Hz) On the Floor of Monterey Bay

by

Edmund J. Chaffee
Lieutenant, United States Navy
B.S. in Physics, University of Washington

Submitted in partial fulfillment of the
requirements for the degree of

MASTER OF SCIENCE IN PHYSICS

from the

NAVAL POSTGRADUATE SCHOOL

December 1979

ABSTRACT

Using a Cs vapor magnetometer, fluctuations of the total magnetic field in the .01 Hz to 3 Hz frequency range were observed on the floor of Monterey Bay, California. Fourteen hours of data were recorded over a period of six months in 1979 at several depths from 30 to 300 meters. A small, inexpensive recording system was designed and manufactured having a noise floor below 10^{-3} nT in the frequency range of interest. Data analysis includes an ocean wave/geomagnetic fluctuation comparison along with a qualitative analysis of the power spectra of the fourteen hours of geomagnetic fluctuation data. Typical geomagnetic fluctuation spectrum levels were found to be about 1 $(nT)^2/Hz$ at .01 Hz. As the frequency increased, the magnitude of the spectrum decreased to approximately 10^{-5} $(nT)^2/Hz$ at 3 Hz. Correlation between ocean wave period and peaks in the geomagnetic fluctuation spectra was observed.

TABLE OF CONTENTS

LIST OF ILLUSTRATIONS

ACKNOWLEDGEMENT

Although many people contributed directed and indirectly to this thesis, I owe a special gratitude to Dr. Otto Heinz and to Dr. Paul Moose, my advisors for this experiment. For their guidance, assistance, and most of all, their infectious enthusiasm, I am sincerely grateful.

I am also greatly indebted to Mr. Robert Smith and to Mr. William Smith of the Research Department for their technical expertise in converting general ideas into high quality performance electronics equipment. Also, their knowledge and skill in overcoming the problems associated with electrical interconnections in a deep ocean environment was invaluable to the success of this endeavor. For this, and the many long hours assisting in the data gathering, I offer my sincere thanks.

I would also like to thank Mr. Thomas Maris of the Physics and Chemistry Department for his conception, design, and manufacture of the support stands for the sensor and sensor electronics. His inventiveness and knowledge of the practical considerations associated with shipboard handling constraints resulted in an extremely effective and easily handled system.

I am greatly appreciative to Captain Woodrow Reynolds and the crew of the Research Vessel Acania for their expert handling in launching and retrieving the data gathering equipment.

Finally, I would like to thank my wife, Virginia Chaffee, for putting up with the long hours and converting my illegible scratchings into a readable manuscript.

I. INTRODUCTION

A knowledge of the ambient magnetic fields and their temporal variations on the ocean floor is of considerable interest both to basic geophysics and a number of Naval applications. Several operational Navy systems such as M (agnetic) A (nomaly) D (etection), magnetic mines, torpedoes, as well as projected systems (such as ELF communication systems) are based on the detection of small changes in the magnetic field in the ocean. With the advent of superconducting magnetometers, the ability to detect extremely small field variations ($<10^{-5}$ nT) is realized, and it has become evident that detailed experimental data on the ambient geomagnetic field in the ocean is necessary to determine the noise environment that detectors will be operating in. In particular, a study of the geomagnetic variations below 100 Hz is of particular interest. Above 100 Hz the attenuation in sea water is too great to make systems operating at these frequencies practical. From a scientific point of view, the study of the time-varying component of the earth's magnetic field and its propagation in the ocean floor is of interest in gaining a better understanding of basic geophysical processes, such as the conductivity of the oceanic crust, internal ocean waves, and coastal current systems.

In previous work [Clayton, 1978], the power spectrum of the fluctuations on land were measured in Monterey, California in the .1 to 40 Hz range. These results were used as a

comparative data base for the ocean floor measurements. Data was recorded on the floor of Monterey Bay at depths from 100 to 1000 feet over a period of several months. These shallow water ocean measurements provide both a preliminary look at typical variations that can be expected as well as a means to test and evaluate the sensing and recording systems that will be utilized in planned deep ocean measurements. A total of fourteen hours of geomagnetic field recordings were made at various times of the day. Frequency analysis was performed on the data yielding the power spectrum of the fluctuations in the frequency range from .01 to 3 Hz. In addition, ocean wave data was recorded from a surface buoy concurrently with one hour of geomagnetic variations on the ocean floor and in the same general location.

II. BACKGROUND

A. SOURCES OF GEOMAGNETIC FLUCTUATIONS

Figure 1 shows an approximate power spectrum of the fluctuations measured on the earth's surface having a period of a day or shorter. Current systems generated in the upper atmosphere by solar heating are responsible for the major diurnal variations (24 hour period). Magnetic storms also have their main frequency components in the same region of the spectrum and their occurrence appears to be closely associated with the solar sunspot cycle. Magnetic storms are believed to be generated by the changing pressure of the solar wind on the outer boundary of the geomagnetic field and the response of the magnetosphere to these changing external pressures.

Geomagnetic variations below a few hertz are typically referred to as micropulsations. These are divided into two types: continuous or pc and irregular or pi. They are further divided according to their periods, the longest being pc5, down to the shortest periods (pc1 or pi1, see Figure 1). Pc's last for several hours while the pi's duration may vary from a few minutes to about one hour. It is believed that micropulsations result from wave-particle interaction in the magnetosphere [Jacobs 1970]. Above 3 Hz, the most pronounced geomagnetic field variations are the earth-ionosphere cavity resonances (Schuman resonances), which result from disturbances resonantly excited by

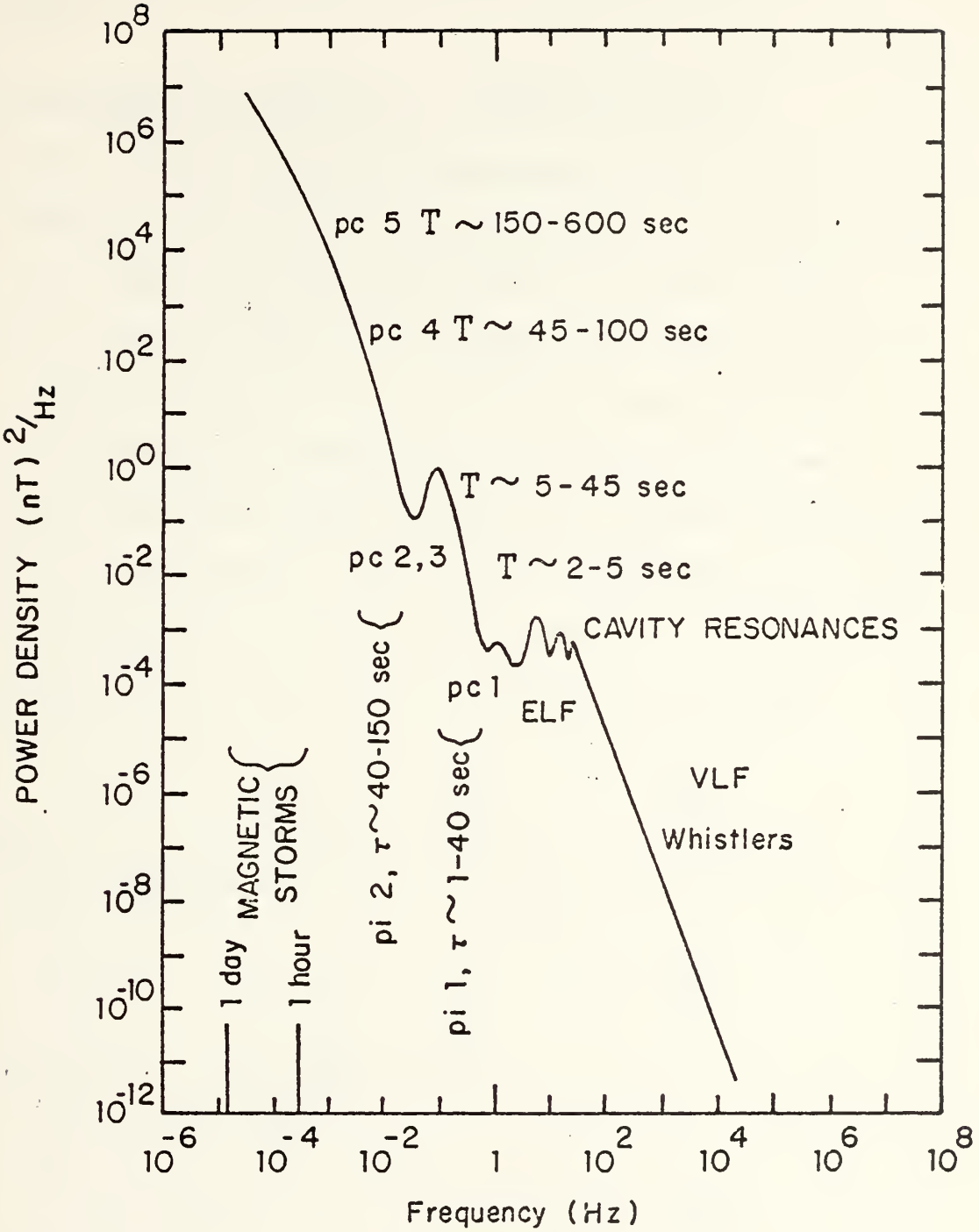

Figure 1

Power Spectrum of Geomagnetic Disturbances Observed on the Surface of the Earth.

[Cladis, Davidson, and Newkirk 1971]

lightning transients in the concentric spherical cavity bounded by the earth and the ionosphere [Schumann and König, 1954].

B. ELECTROMAGNETIC PROPAGATION IN CONDUCTING MEDIA

In order to predict expected geomagnetic field variations, it was necessary to examine the propagation of electromagnetic waves in the ocean including the effect of the sea bottom where the data was recorded. The model used for these calculations is shown in Figure 2. γ is the propagation constant, and η is the intrinsic impedance. Sea water and the sea bottom can be considered good conductors at these frequencies while air is a dielectric. It is also assumed that the three media are non-magnetic ($\mu_1 = \mu_2 = \mu_3 = \mu_0$).

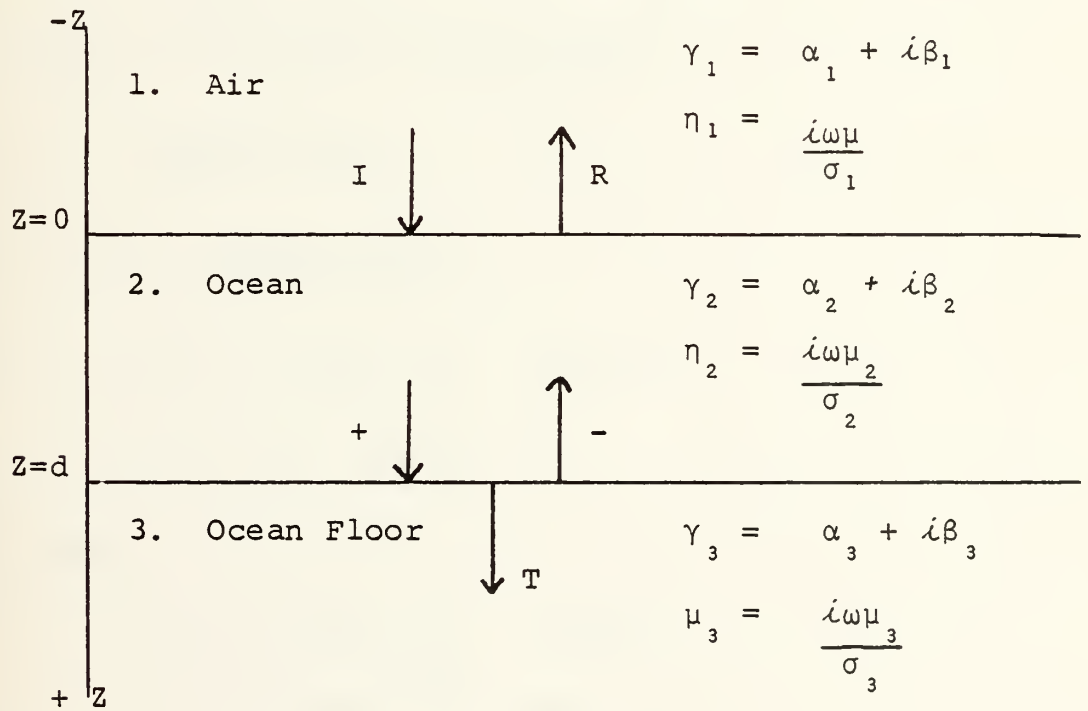

Figure 2.

Electromagnetic Propagation in a three layer medium (Plane Waves)

Based on the above the following approximations are made:

1. Air: $\gamma_1 = i\omega(\mu_1 \varepsilon_1)^{\frac{1}{2}}$

$$\eta_1 = \left(\frac{\mu_1}{\varepsilon_1}\right)^{\frac{1}{2}}$$

2. Sea Water: $\gamma_1 = (i\omega\mu_2\sigma_2)^{\frac{1}{2}}$

$$\eta_2 = \left(\frac{i\omega\mu_2}{\sigma_2}\right)^{\frac{1}{2}}$$

3. Sea Bottom: $\gamma_2 = (i\omega\mu_3\sigma_3)^{\frac{1}{2}}$

$$\eta_3 = \left(\frac{i\omega\mu_3}{\sigma_3}\right)^{\frac{1}{2}}$$

$\mu_1 = \mu_2 = \mu_3 = \mu_0 = 4\pi \times 10^{-7}$ henry/meter

$\varepsilon_1 = 81\varepsilon_0 = 7.2\times10^{-12}$ farad/meter

$\sigma_2 = 4$ siemens/meter

$\sigma_3 = 10^{-1}$ siemens/meter

1. Air: $|\gamma_1| = 1.9\times10^{-8} f$ meters^{-1}

$|\eta_1| = 377$ ohms

2. Sea Water:

$|\gamma_2| = 5.6\times10^{-3} f^{\frac{1}{2}}$ meters^{-1}

$|\eta_2| = 1.4\times10^{-3} f^{\frac{1}{2}}$ ohms

3. Sea Bottom:

$|\gamma_3| = 8.9\times10^{-4} f^{\frac{1}{2}}$ meters^{-1}

$|\eta_3| = 8.9\times10^{-3} f^{\frac{1}{2}}$ ohms

For this treatment, only perpendicular incidence of plane T.E. (transverse electric) or T.M. (transverse magnetic) waves are considered. For the magnitude of the propagating wave, the inclusion of other angles of incidence on the air/sea boundary is a simple matter of cosine of the angle dependence. Regardless of angle of incidence, the direction of propagation will always be vertically downward.

With the above considerations, the wave equations in the three media are as follows:

Region 1: $Ex_1 = E_i e^{-\gamma_1 z} + E_r e^{\gamma_1 z}$

$$By_1 = \frac{\mu_o}{\eta_1} (E_i e^{-\gamma_1 z} - E_r e^{\gamma_1 z})$$

Region 2: $Ex_2 = E_+ e^{-\gamma_2 z} + E - e^{\gamma_2 z}$

$$By_2 = \frac{\mu_o}{\eta_2} (E_+ e^{-\gamma_2 z} - E_- e^{\gamma_2 z})$$

Region 3: $Ex_3 = E_t e^{-\gamma_3 z}$

$$By_3 = \frac{\mu_o}{\eta_3} E_t e^{-\gamma_3 z}$$

Boundary Conditions:

At $z = 0$ $\quad E_i + E_r = E_+ + E_-$

$$\frac{\mu_o}{\eta_1} (E_i - E_r) = \frac{\mu_o}{\eta_2} (E_+ - E_-)$$

At $z = d$ $\quad E_+ e^{-\gamma_2 d} + E_- e^{\gamma_2 d} = E_t e^{-\gamma_3 d}$

$$\frac{\mu_o}{\eta_2} (E_+ e^{-\gamma_2 d} - E_- e^{\gamma_2 d}) = \frac{\mu_o}{\eta_3} E_t e^{-\gamma_3 d}$$

Assuming $\eta_2 << \eta_1$ and $\eta_3 << \eta_1$, after considerable algebra yields.

$$By_2(z) = 2Bi \frac{(q+1)e^{\gamma_2(d-z)} - (q-1)e^{-\gamma_2(d-z)}}{(q+1)e^{\gamma_2 d} - (q-1)e^{-\gamma_2 d}}$$

where $q = \frac{\eta_3}{\eta_2} = \left(\frac{\sigma_2}{\sigma_3}\right)^{\frac{1}{2}}$

$$By_2(d) = \frac{4Bi}{(q+1)e^{\gamma_2 d} - (q-1)e^{-\gamma_2 d}}$$

Substituting the calculated values for η_2, η_3 and γ_2 yields

$$By_2(d) = \frac{4Bi}{7.3e^{5.6x10^{-3}f^{\frac{1}{2}}d} - 5.3e^{-5.6x10^{-3}f^{\frac{1}{2}}d}}$$

Following is a plot of values for By_2 vs. depth for various frequencies (Figure 3).

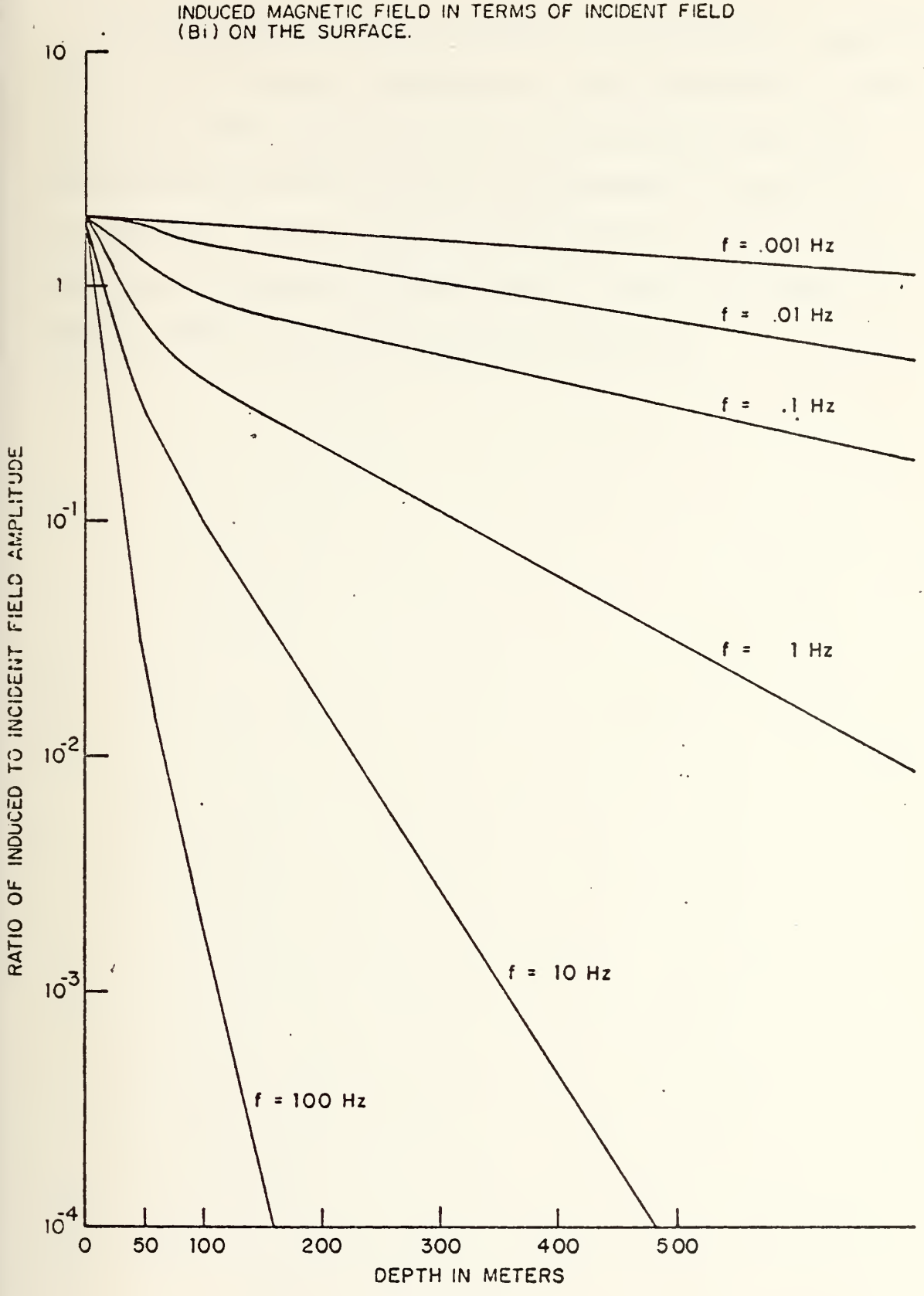
INDUCED MAGNETIC FIELD IN TERMS OF INCIDENT FIELD (Bi) ON THE SURFACE.
10
1
10^{-1}
10^{-2}
10^{-3}
10^{-4}
RATIO OF INDUCED TO INCIDENT FIELD AMPLITUDE
f = .001 Hz
f = .01 Hz
f = .1 Hz
f = 1 Hz
f = 10 Hz
f = 100 Hz
0
50
100
200
300
400
500
DEPTH IN METERS

Figure 3.

By examining Figure 3, it is seen that at any appreciable depth (>100 meters), geomagnetic field variations of frequencies above 100 Hz will be greatly attenuated, and undetectable for the Cs vapor magnetometer (sensitivity $\approx .005$ nT). It can also be seen that at very low frequencies and shallow depths, the amplitude of the variations are approximately twice the incident amplitude.

C. OCEAN WAVE PRODUCED MAGNETIC FLUCTUATIONS

Aside from externally produced geomagnetic fluctuations (external to the ocean), internally produced magnetic fluctuations occur due to ocean water movement (movement of a conductor in an external B field). For a first approximation only surface waves need to be considered. Figure 4 is a plot of induced magnetic field per meter amplitude of surface wave for several wave periods [Weaver 1965].

The plot of induced magnetic fields is based on an inclination angle of the earth's main field of 70 degrees (Monterey, CA I=62 deg.) and the surface wave propagating along the magnetic meridian (θ=0 deg.). As is seen on the plot, one meter high waves produce magnetic variations of the order of 1nT at depths up to 100 meters in the frequency range that one would expect for surface waves (T=12 sec.). In Weaver's treatment, an infinite ocean depth was assumed. In generalizing Weaver's equations to incorporate bottom reflection and transmission, it was found that the effect of the bottom decreased the magnitude of the induced magnetic field by less than 3 dB in the frequency range of interest (T<60 sec.) in water depths less than 500 meters. There exists experimental evidence in confirming this prediction [Wynn and Trantham 1968]. For wave periods of less than 20 seconds and at depths greater than a few hundred meters, the effect of the bottom becomes negligible.

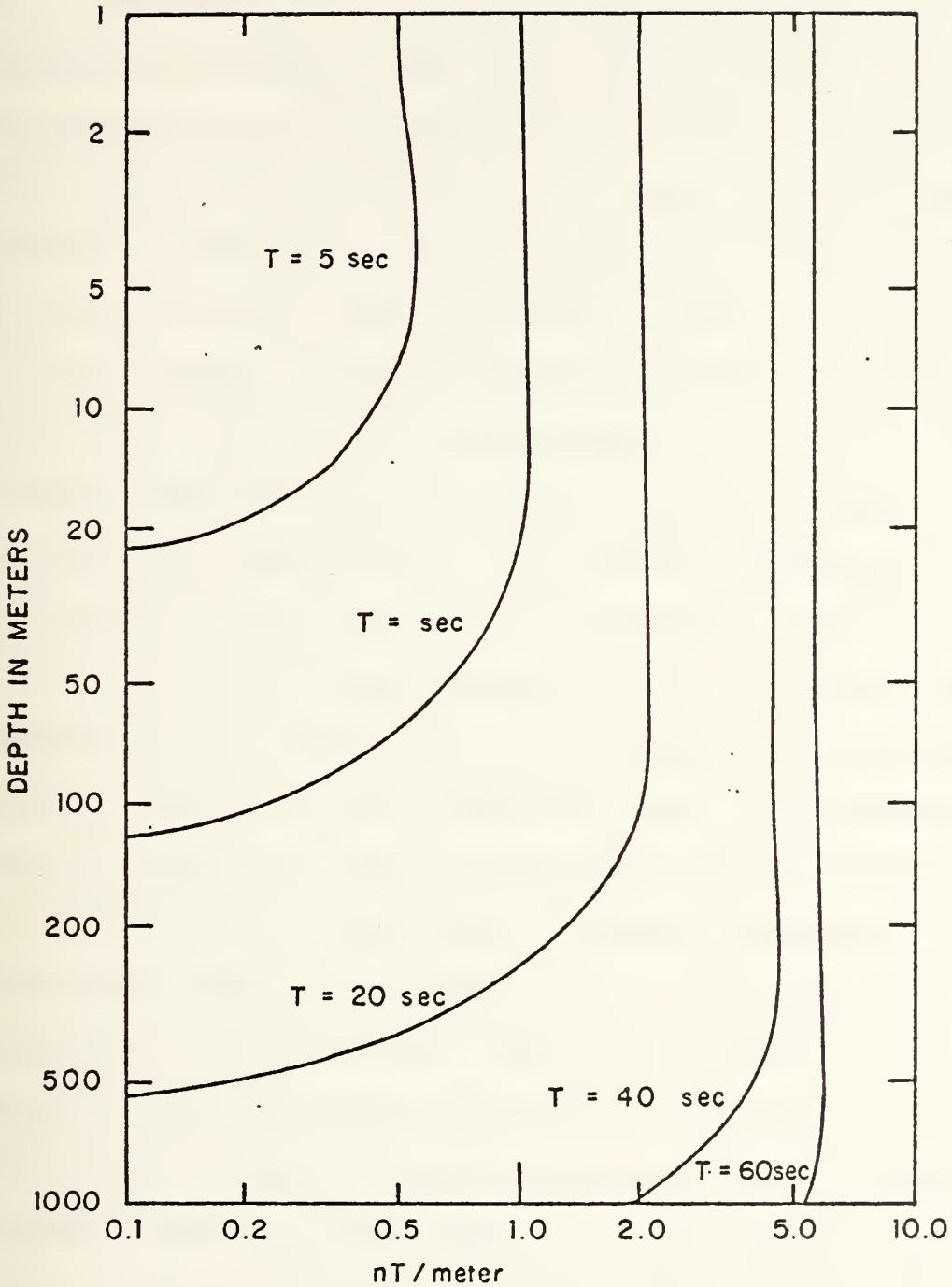

Figure 4.

Induced Magnetic Field per Meter Amplitude of the Surface Wave.
[Weaver 1965]

D. REVIEW OF EARLIER WORK

There exist several studies of low frequency (less than 100 Hz) geomagnetic variations on land. Previous work by Santirocco and Parker (1963) and Parker (1964) indicate that the geomagnetic field decreases with a slope of approximately -6dB/octave between 10^{-4} and 1 Hz. From 1 to 40 Hz the field exhibits a leveling off and is dominated by Schumann Resonances [Schumann and Konig 1954]. At about 80 Hz, the sharp decrease in slope resumes. Several references concerning similar studies are listed in the bibliography.

Recent work was done in the low frequency range (.1 to 14 Hz) [Smith and Buxton 1975]. In La Mesa, Monterey, California work has been done in the .1 to 10 Hz range [Barry 1978] and in the .1 to 40 Hz range [Clayton 1979]. The work in Monterey was done both to investigate the low frequency variations and to set up a base line for comparison with the geomagnetic variation recordings made on the ocean floor in this experiment. There exists little data on actual geomagnetic noise measurements taken on the ocean floor in the frequency range of interest (.001 to 10 Hz). Most studies done in this frequency range have been experiments to study the geomagnetic fluctuations produced by surface waves and their correlation. Generally, these have been done in a very shallow depths ($<$50 meters) [Wynn and Trantham 1968] and [Clark, Allen and Johnson 1979].

III. EXPERIMENTAL SETUP

A. GENERAL LAYOUT OF EXPERIMENT

The measurement of the geomagnetic field variations was carried out with a Cesium vapor, optically pumped magnetometer. The sensor and sensor electronics were housed in a glass sphere which was in turn rigidly mounted to a non-metallic, non-magnetic stand. This stand rested on the ocean floor and two hundred feet above it floated two additional spheres that housed the power supplies (gell-cell batteries), electronics equipment, and dual-channel analog cassette recorder. These spheres were electrically connected to the sensor by means of a 200 foot coaxial cable (see Figure 5).

The time varying geomagnetic field was recorded during six days from May through September 1979: 4/20/79, 5/10/79, 7/16/79, 7/17/79, 9/17/79, and 9/18/79. The first two days of data (5 hours recording time) were recorded with a preliminary recording system sensitive to approximately .1 Hz. The second two days data (5 hours recording time) were recorded with an expanded system with increased frequency band coverage to about 1 Hz. The final two days data (4 hours recording time) were recorded with the expanded system with an additional 20 dB amplifier that expanded the coverage out to a few Hz. The recording systems are described in detail in part B of this section.

SCHEMATIC OF EXPERIMENTAL LAYOUT FOR SHALLOW WATER MAGNETOMETER MEASUREMENT

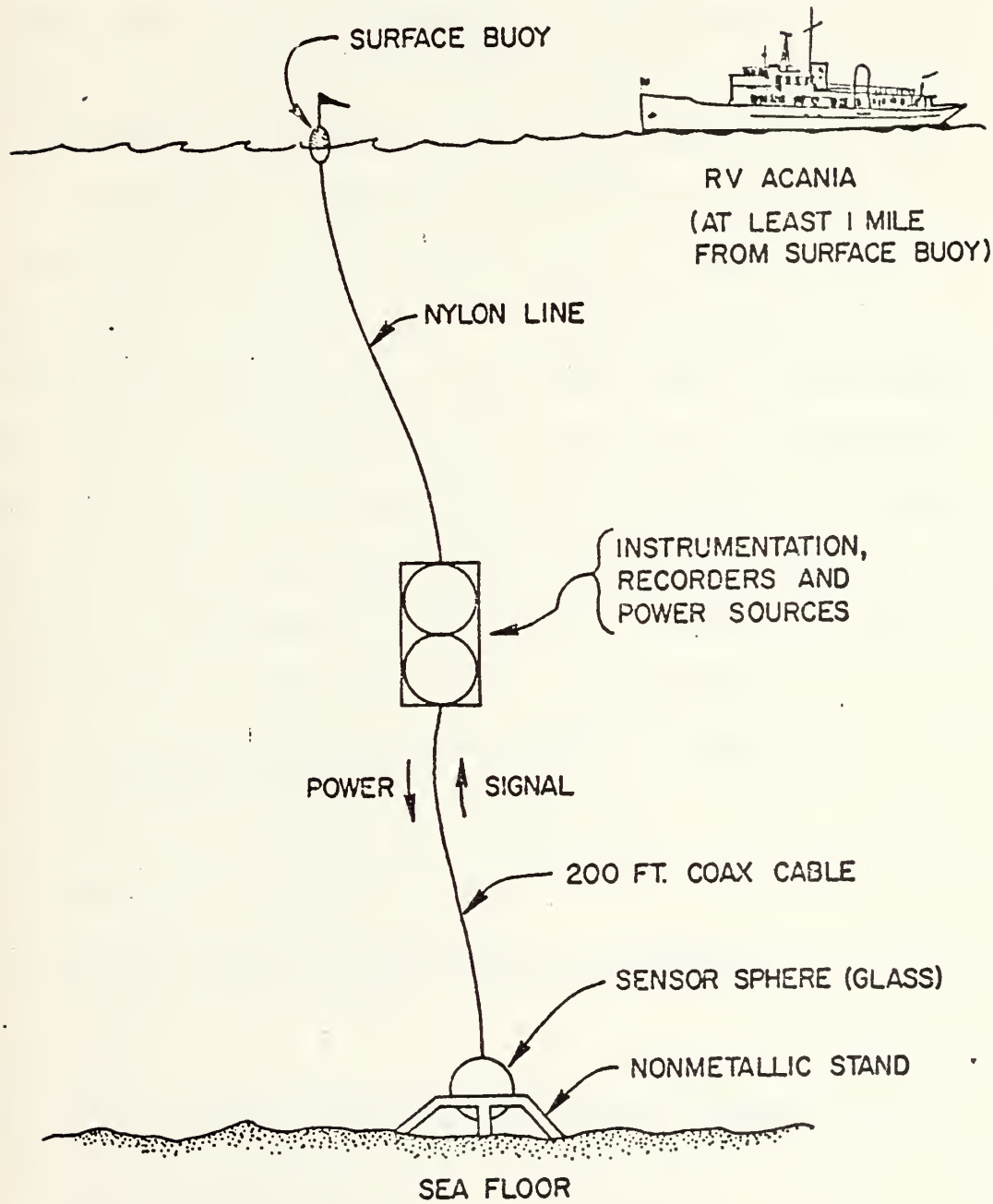

Figure 5

B. DATA COLLECTION SYSTEM

In order to obtain data on the low frequency geomagnetic variations on the floor of Monterey Bay, it was necessary to design a suitable measurement and recording system that could be used in an ocean environment subject to constraints such as low power, small size, non-metallic and non-magnetic housings, high sensitivity, and wide frequency band coverage. After the first five hours of data were analyzed, improvements were made to the recording system for the second five hours of data collection (7/16/79, 7/17/79). As a result of the subsequent data analysis, further improvements were incorporated into the system for the last four hours of measurements.

The system used for the first five hours of measurement is described below. Following this description is a section on the improvements made that were incorporated for the last nine hours of measurement. The original system illustrated in Figure 6 has the following major components:

1) Cesium Vapor Sensor (Varian Model 4938) and Sensor Electronics

2) Sensor Coupler (Varian Model 4938)

3) Reference Oscillator-2KHz

4) Analog Cassette Tape Recorder-2 Channel (Morantz Model CD330)

5) Mixer

6) Discriminator-Frequency to Voltage (Anadex P-375)

7) DC Power Supplies (+30, +24, $\pm$12, +6) (Gould Gelyte Cells)

The sensor generates a signal whose frequency is proportional to the ambient magnetic field intensity. The

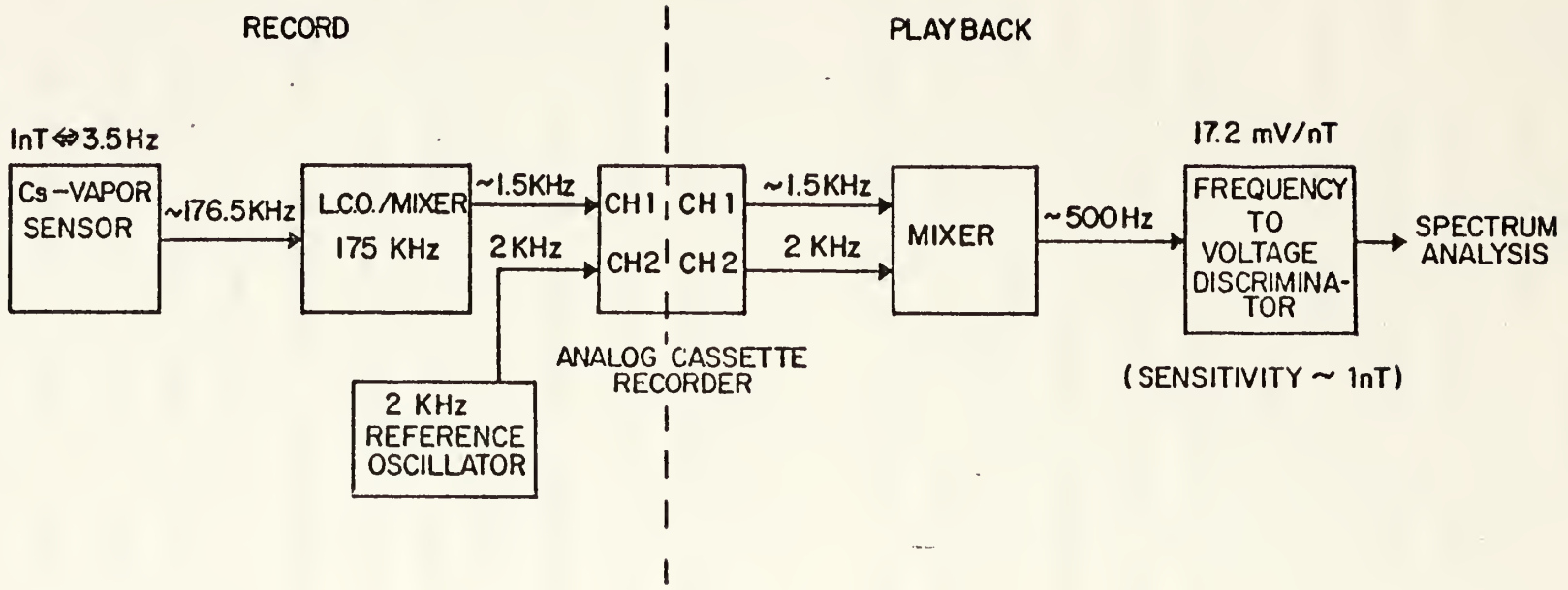

SYSTEM WITH RECORDER (WITHOUT VOLTAGE CONTROLLED OSCILLATOR)

Figure 6

frequency (called the Larmor frequency) is approximately 176.5KHz in the Monterey area. The signal is transmitted via coaxial cable to the sensor coupler, where it is mixed with a 175KHz crystal oscillator signal and generates a difference frequency between 0 and 2000 Hz. This mixer output is sent to one channel of the analog cassette recorder. The other channel has a 2KHz reference frequency recorded on it. When the tape is played back, the two output channels are sent to a mixer that generates a difference frequency. The difference frequency is sent to the frequency-to-voltage discriminator and its output (0-10VDC) is sent to the spectrum analyzer.

The system components are discussed in the following subsections:

1) Sensor, Cesium Vapor Magnetometer - The sensor acts as oscillator producing a signal whose frequency, (Larmor frequency), is directly proportional to the total magnetic field intensity in which the sensor operates. This proportionality is a direct result of the magnetic field dependence of the Zeeman splitting of the energy levels of the Cesium valence electron. The energy levels have a number of sublevels whose energy differences are proportional to the intensity of the external magnetic field. The separation in energy (ΔE) between these Zeeman levels can be calculated by measuring the frequency (ν) of the emitted or absorbed photons since $E=h\nu$. But ΔE is also directly proportional to the ambient magnetic field as shown by the equation:

$$\Delta E = \frac{geh}{4\pi m} B \quad \text{where}$$

g = Landè g factor

e = charge on the electron

h = Planks' constant

m = mass of the electron

B = magnetic field strength

Thus, by measuring ν, the magnetic field intensity B can be measured via a proportionality constant. A detailed description of the optically pumped magnetometer can be found in Bloom [1961] and Barry [1978].

The sensor used in our experiment had the following characteristics:

a) Sensor output proportionality constant: 3.499 Hz/nT

b) Sensitivity: 5 picotesla

c) Range: Continuous from 20,000 to 80,000 nT

d) Nominal Field Frequency: $\approx$176500 Hz ($\approx$ 50,440 nT)

The sensor was securely fastened inside a glass sphere which was tested to 15,000 psi external pressure. The sphere in turn was mounted in a plastic, sand weighted support stand that would sit level on the ocean floor.

It was necessary to have a completely non-metallic housing and support stand to avoid electrolytic currents that might arise from a metal in the ocean. Such currents can produce magnetic noise capable of contaminating the data. Inside the sphere, the sensor axis was mounted vertically. This allowed the ambient geomagnetic field vector

(Inclination angle 62^{o}) to fall within the optimum operating cone of the sensor.

The sensor was connected to the sensor coupler by a 200 foot coaxial cable. The sensor coupler and the electronics associated with the recording system were housed in two glass spheres that were rigidly mounted in an aluminum frame. This package (tied to the sensor stand with nylon line) was 50 pounds positively buoyant and floated 200 feet above the sensor (see Figure 5). The sensor with support stand was 150 pounds negatively buoyant resulting in an overall 100 pound negatively buoyant system.

2) Sensor Coupler - the sensor coupler's purpose was to provide power to the sensor and the sensor electronics package and receive the Larmor frequency from the sensor (along the same 200 foot coaxial cable). The coupler used in this experiment had a reference crystal oscillator of 175KHz which was beat with the Larmor frequency in a mixer circuit giving an output signal that was a sine wave with a frequency equal to the difference between the Larmor frequency and the reference oscillator frequency. Inside the coupler sphere there was also a 30VDC gell-cell battery pack to provide power for the coupler and sensor. The output of the mixer was fed through electrical penetrators to the adjoining sphere that housed the cassette recorder.

3) Reference Oscillator (2KHz) - It was found that by using a reference signal on one channel of the cassette recorder and the data signal on the other channel and mixing

their output, the noise of the tape recorder could be reduced by 10 dB. To achieve this, a 2 KHz reference oscillator was designed. The oscillator uses a 20 KHz crystal and frequency divides it to produce a 2 KHz sine wave output. It is powered by a 6 VDC battery. The circuit schematic is shown in Appendix A.

4) Analog Cassette Recorder - In order to meet the size constraints (15 inch inner diameter-glass sphere) and also be of relatively low cost (under $300.00), the Morantz CD 330 Cassette two channel recorder was selected. It was powered by a 6 VDC gell-cell. The tape recorder had the following characteristics:

a) speed: 1-7/8 ips

b) frequency range: 40 Hz to 12 KHz

c) dual channel

d) Wow and Flutler: .12%

5) Mixer - the mixer circuit designed for this experiment was powered by $\pm$12 VDC. The 2 KHz reference frequency was mixed with the sensor coupler output frequency (varying around 1.5 KHz) to produce a difference frequency (0-1000 Hz). The circuit also included a low pass filter on the output with a cutoff at 1 KHz. This difference frequency was then fed into the discriminator to obtain an analog voltage. The schematic for the mixer circuit is shown in Appendix A.

6) Discriminator (Anadex PI-375) - The discriminator was a 24 VDC frequency to analog voltage converter with the following characteristics:

a) Input frequency range: 0-2000 Hz

b) Output DC voltage: 0-10V full scale

c) Power: 22-30 VDC

d) Conversion Factor (0-10 Hz) - 17.2mV per 1nT (3.499 Hz)

The discriminator had an internal low pass filtering circuit that began to cut off at 10 Hz and fell off by 24 dB at 100 Hz. The output of the discriminator was then fed into a spectrum analyzer.

7) DC Power Supplies: (+30 VDC, +24 VDC, $\pm$12 VDC, +6VDC)- Gould Gelyte sealed rechargeable lead batteries were used as the power sources. The size and ampere-hour ratings varied as to the type of load. Power considerations were a major problem due to the high current requirements of the sensor ($\approx$ 1 AMP) and the recorder ($\approx$ ½ AMP). For long term measurement on the ocean floor, this remains a problem and is addressed in the conclusion of this thesis.

The improved data collection system is illustrated in Figure 7. As shown in this figure, it is essentially the same as the previous system with the addition of two more stages: the discriminator and voltage controlled oscillator (VCO). The discriminator was the same on as described previously. The output of the sensor coupler (nominally 1.5 KHz) is fed into the discriminator producing an analog voltage which is then AC coupled to the voltage controlled oscillator via a pre-amplifier. The output of the voltage controlled oscillator is a sine wave of varying frequency centered at 1.5 KHz. The amount of frequency variation is

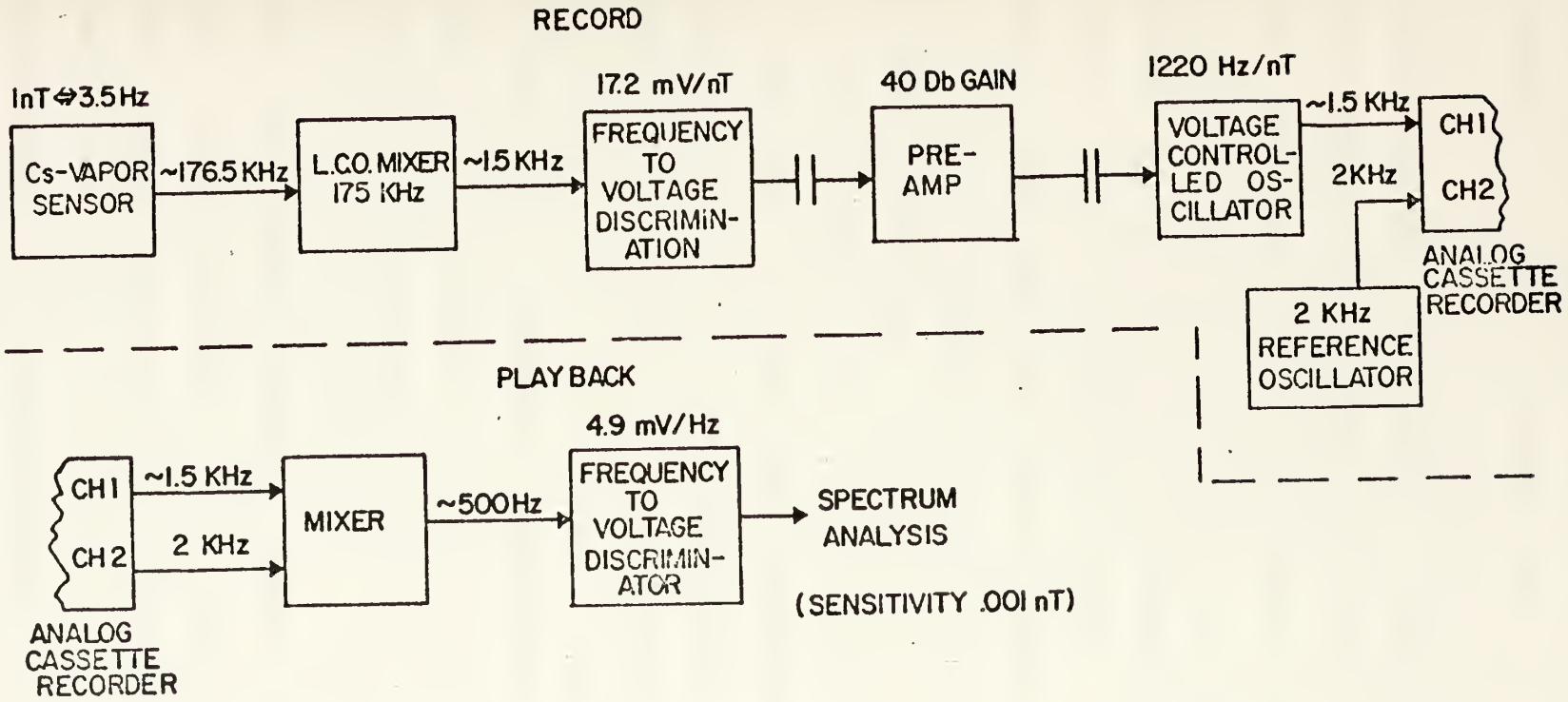

EXTENDED RANGE SYSTEM (WITH VOLTAGE CONTROLLED OSCILLATOR)

Figure 7

dependent upon the amplitude of the voltage at the input. The output of the VCO is then fed into one channel of the tape recorder and is later processed in the same manner as the original system. The effect of adding this additional equipment changes the frequency conversion to approximately 122 Hz/nT vice the 3.499 Hz/nT in the original system. The AC coupling is necessary to prevent the large amplitude ELF geomagnetic variations ($f<.1$ Hz) from overdriving the system as a result of its increased sensitivity. The transfer function for this improved system is shown in Figure 8. This transfer function represents the gain of the entire system up to the spectrum analyzer. The fall off at the low frequency end of the spectrum is due to the AC coupling prior to the VCO and the fall off at the high frequency end is due to the low pass filtering in the two discriminator stages (one in the recording section and one in the playback section). The circuit design for the VCO is given in Appendix A. The circuit includes an additional pre-amplifier (20 dB gain). This extra gain stage was not used to record the second five hours of data because it was thought that the low frequency geomagnetic variations generated by the ocean waves would overdrive the recording system in shallow water. After analysis, it was determined that the additional 20 dB gain could be used and thus the last 4 hours recorded used this extended system. With the additional gain, the frequency conversion factor became approximately 1220 Hz/nT. The transfer function for the extended system is shown in Figure 9. As is seen, the extended system transfer function

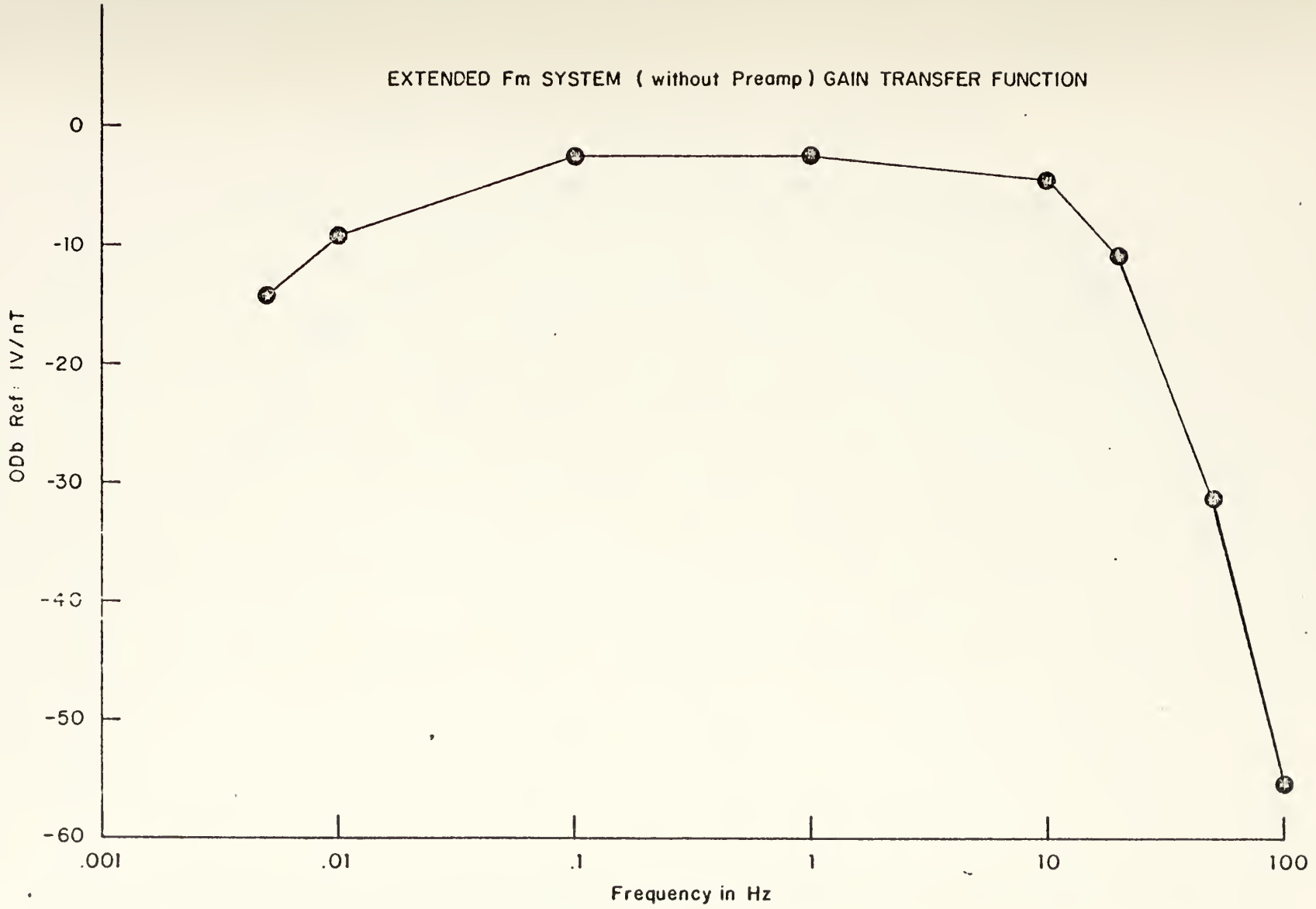
EXTENDED Fm SYSTEM (without Preamp) GAIN TRANSFER FUNCTION
0
-10
-20
-30
-40
-50
-60
ODb Ref: 1V/nT
.001
.01
.1
1
10
100
Frequency in Hz

Figure 8.

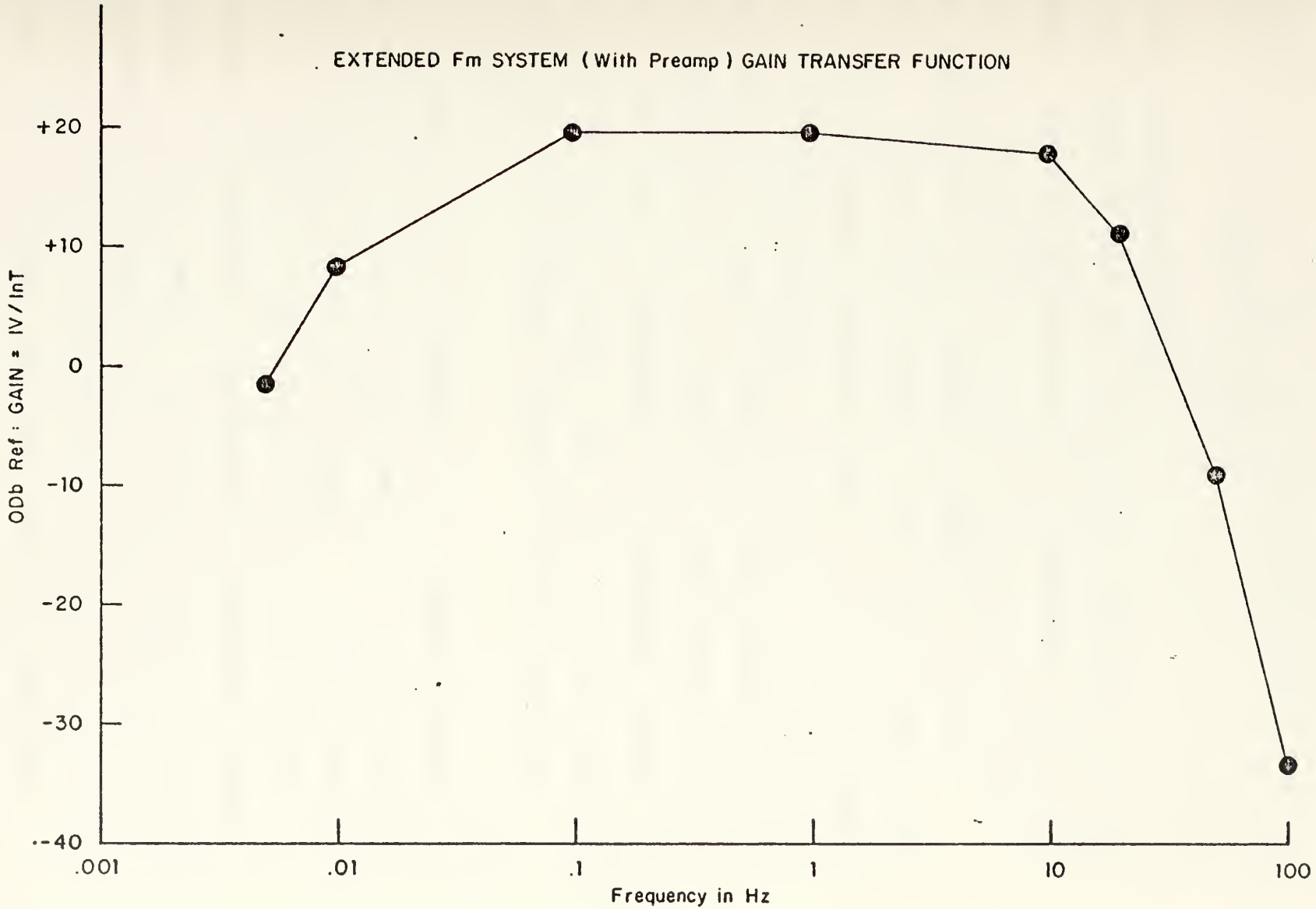
EXTENDED Fm SYSTEM (With Preamp) GAIN TRANSFER FUNCTION
+20
+10
0
-10
-20
-30
-40
ODb Ref: GAIN = 1V/1nT
.001
.01
.1
1
10
100
Frequency in Hz

Figure 9.

is the same as that shown in Figure 8 with the addition of 20 dB of gain. There is slightly more filtering at the low frequency end of the band due to additional capacitive coupling in the pre-amplifier stage.

C. DATA ANALYSIS EQUIPMENT

The spectrum analyzer used for this experiment was the Nicolet Scientific Corporation Mini Umbiquitous (Model 440B). This spectrum analyzer is a fully-digitalized instrument that provides real time spectrum component analysis of analog or digital input signals in 400 spectral bins across one of 16 selectable frequency bands. The result of each of the 400 independent analyses performed by the instrument is displayed on an internal Cathode Ray oscilloscope as a dot indicating the power and frequency. The bandwidth of each line of resolution is dependent on the maximum frequency of the selected analysis range. The 400B translates time domain signals into the frequency domain by Fourier transform techniques.

The analyzer has an option of two "window functions" for application to the data in the time domain, as an amplitude function multiplying the data samples. In effect the entire analysis sequence is amplitude modulated by the window function and the result transferred to the Digital Fourier Transform analysis memory. The window function is unity for the rectangular window and for the Hanning function; it is $\sin^2 n/1024$ where "n" represents the position of the sample in the 1024 data block. The later weighting function

provides for a sharper rolloff of the signal sidelobes in the frequency domain, due to the finite length of the input signal, than that provided by uniform weighting. The Hanning window was used for data analysis in this experiment.

The first 5 hours of data were analyzed using the .0025 Hz to 1 Hz frequency band and the second 5 hours of data were analyzed using the .0125 Hz to 5 Hz frequency band. The above frequency maxima were selected because above 1 Hz and 5 Hz respectively, the system noise dominated. The last four hours of data were analyzed using the .025 Hz to 10 Hz frequency band. This band was selected because the sensor sensitivity dominated (set the noise floor) above 10 Hz. Various gain settings and averaging times were used. The gain corrections are incorporated in all of the data plots and the averaging times are noted on the plots.

D. SYSTEM TESTS AND NOISE MEASUREMENTS

A number of system tests were performed prior to data collection and throughout the experiment as changes were incorporated into the system. The Cesium vapor magnetometer was tested with it axis in the vertical direction to determine if this orientation provided the correct output. After numerous measurements, it was determined that vertical orientation provided the correct response provided the sensor axis was within a 15^{o} cone with respect to the vertical axis (this is only true for this geomagnetic latitudes - Inclination angle $\approx 62^{o}$). At geomagnetic latitudes, other than that of Monterey, Ca. (42.5^{o}N), this will not hold due to the change in inclination angle of the earth's main field with respect to the axis of the sensor.

In addition, tests were conducted to see how close the sensor electronics packages could be to the sensor without affecting its output. The results obtained showed the sensor output was not affected providing the electronics package was more than 6" from the sensor.

With the data obtained from these two series of measurements, it was determined that:

1) The sensor could be mounted vertically in the sphere provided the measurements to be taken were conducted in the same general geomagnetic latitude of Monterey, Ca.

2) It was not necessary to orient the sensor in azimuth provided the ocean floor was relatively level (less than 15^{o} inclination).

3) The sensor and sensor electronics could be mounted inside the same sphere provided there was more than 6" separation. (Sensor and sensor electronics were actually 7" apart mounted rigidly on a wood platform inside the glass sphere.)

The noise floor of the sensor itself could not be measured directly. The factory quoted value for sensitivity is .005 nT and this value was used as the "floor" of the system to set the design goal for the associated electronics and recording system. The sensitivity of the sensor is shown as a dashed line on the plots as a separate item to be distinguished from the electronics recording system noise which is also represented on the plots.

The frequency to voltage discriminator was tested to determine the conversion factor and frequency response. First the DC conversion factor was determined with various frequencies applied to the input of the discriminator (0 Hz to 2000 Hz) and the DC voltage was measured at the output. This gave a conversion factor of 17.2m V output per 3.499 Hz (1 nT). To determine the frequency response, the setup in Figure 10 was used.

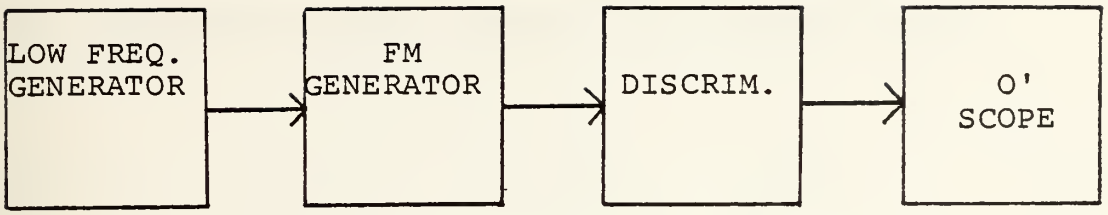

Figure 10

Discriminator Frequency Response Layout

The low frequency (LF) was varied in frequency from .005 Hz up to 100 Hz while maintaining constant amplitude. This varied the FM generator output centered at 1 KHz at varying rates depending on the frequency of the LF generator. This was fed into the discriminator and its output measured on an oscilloscope. The discriminator output was the same frequency as the LF generator. The response was flat up to $\sim$10 Hz and then started to fall off. This attenuation (filtering) at the higher frequencies was incorporated into the discriminator transfer function shown in Figure 12. 0 dB is referenced to 1V/nT where 1nT$\Leftrightarrow$3.499 Hz. It was assumed that below .001 Hz, there was no change in gain and the DC conversion factor of 17.2 mV/nT could be used. As the circuit is designed with a low pass filter, the above is a good assumption.

The sensitivity and frequency response of the Voltage Controlled Oscillator (VCO) and its corresponding amplifier was determined in the following way (see Figure 11).

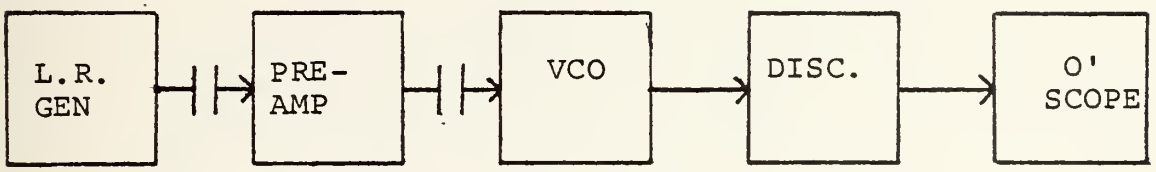

Figure 11

VCO Response Layout

The low frequency (LF) generator was varied in frequency from .005 Hz up to 100 Hz while maintaining a constant input amplitude. This varied the VCO output and subsequently varied the discriminator output at the same frequency as the LF generator. The amount of frequency variation of the VCO is dependent on the voltage amplitude of the applied signal. This was done at several frequencies from .005 Hz to 100 Hz. From this data a gain curve was obtained for the VCO-Discriminator combination over the frequency range of interest (Figure 12). The transfer function is referenced to 0 dB being a gain of 1.

Figure 13 shows the noise spectra of the various system configurations. For each of these measurements a very stable frequency synthesizer (Hewlett Packard Model 3320B) was used to replace the sensor. A constant frequency of 176.5 KHz

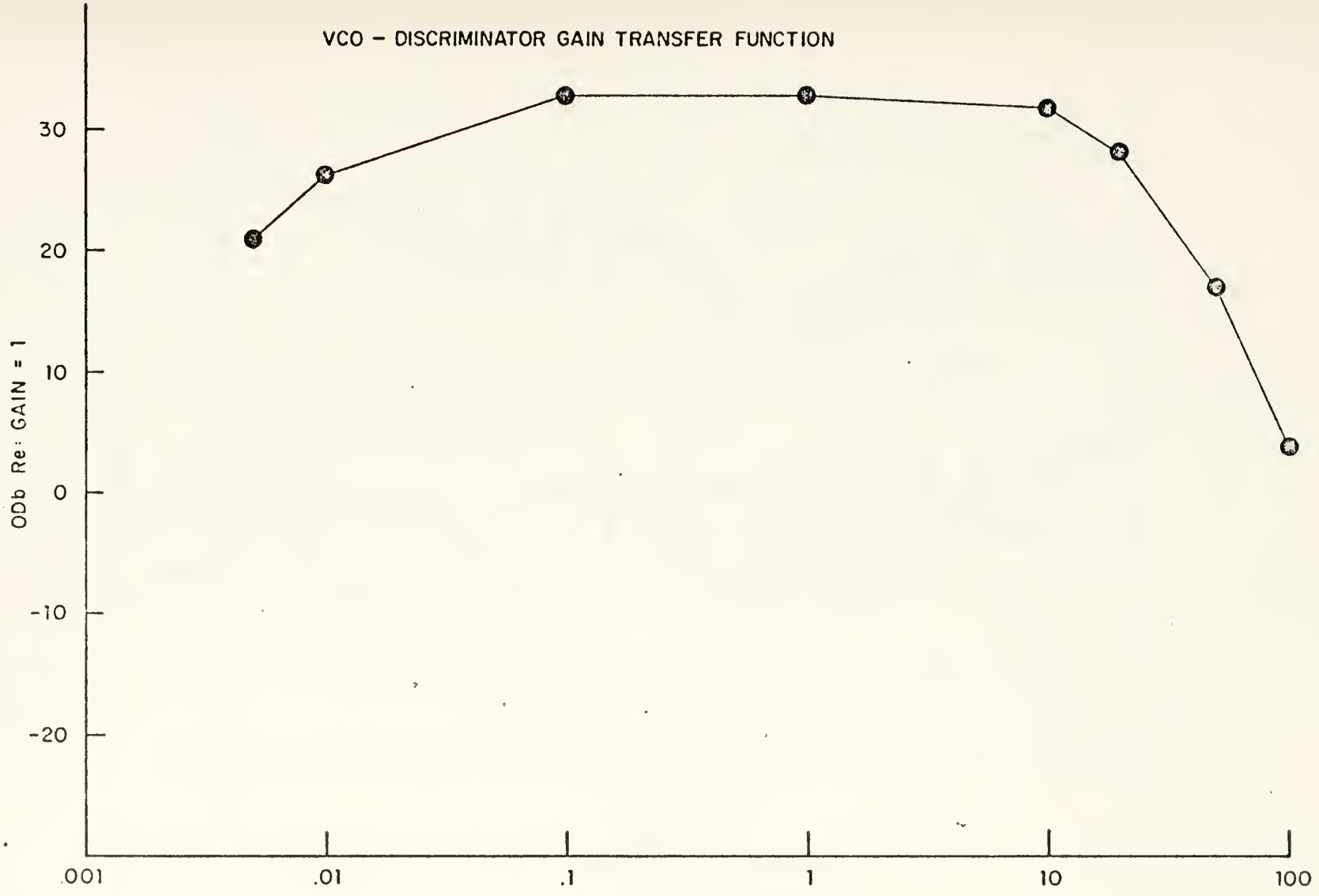
VCO – DISCRIMINATOR GAIN TRANSFER FUNCTION
30
20
10
0
-10
-20
ODb Re: GAIN = 1
.001
.01
.1
1
10
100
Frequency in Hz

Figure 12

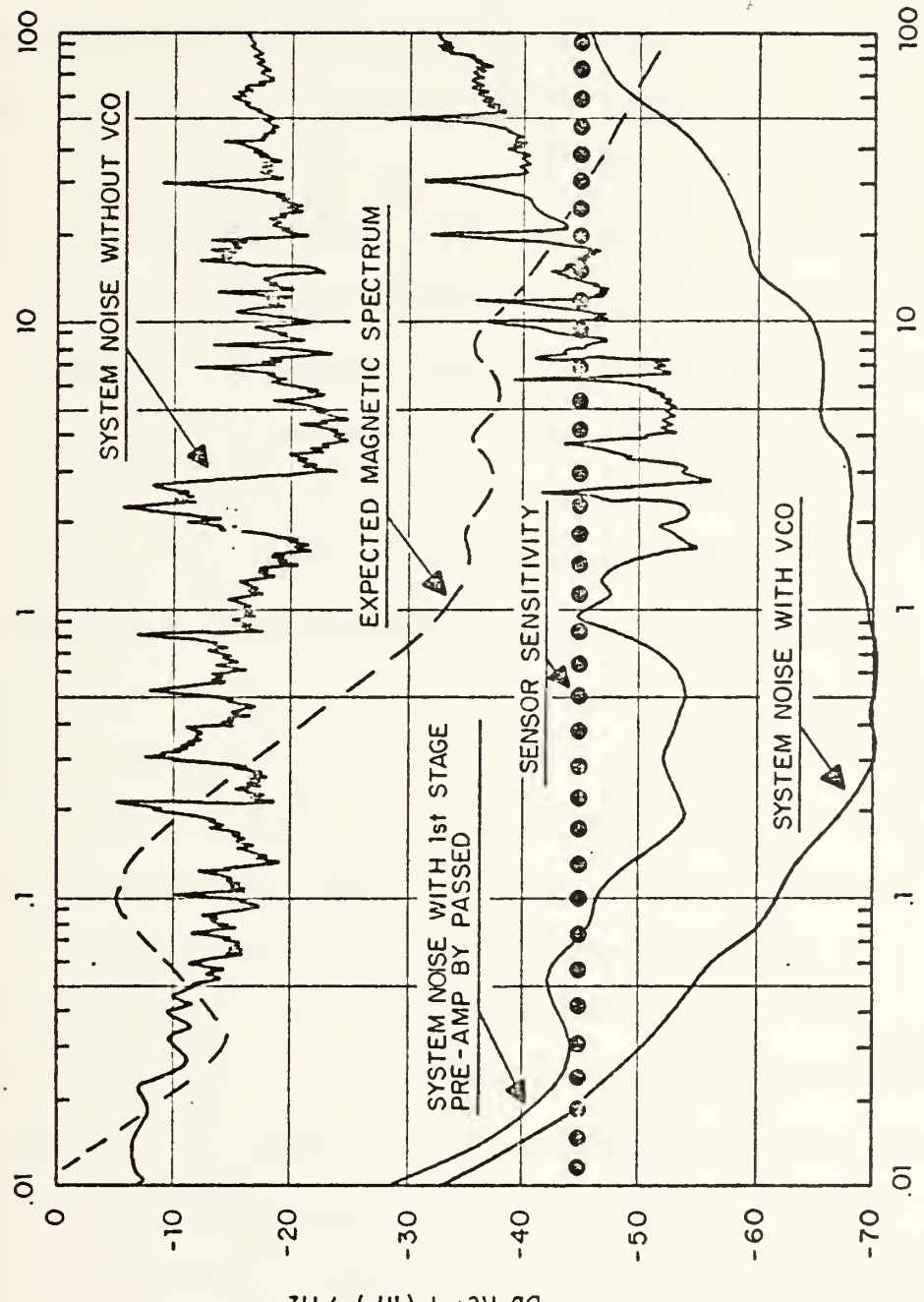

Figure 13
SYSTEM NOISE SPECTRUM

was used to simulate the Larmor frequency into the sensor coupler. From that point on, the system was identical to that used in the actual measurement. By this method it was possible to get an overall system noise measurement of all components with the exception of the sensor itself. The expected geomagnetic spectrum as observed on the surface of the earth is shown in Figure 13 by a dashed line.

The first noise measurement was made on the system shown in Figure 6 but with sensor replaced by the frequency synthesizer. This is labeled "System Noise Without VCO". This high level of noise is generated mostly by the cassette recorder. When compared to the expected magnetic spectrum, it can be seen that the recorder noise completely dominates above .2 Hz, and is confirmed by the data that was taken in the first five hours of measurements.

In an attempt to overcome the recorder noise problem, the VCO was designed (See Figure 7). This has the effect of increasing the signal strength prior to recording and is labeled "System Noise with 1st Stage Pre-Amp Bypassed" in Figure 13. As shown in the figure, this extended the frequency coverage from .2 Hz to about 2 Hz. Above a few Hz, the tape recorder noise again dominated and the data taken (second five hours of measurement) confirmed this.

Finally, an additional 20 dB of gain was added to the VCO. This is labeled "System Noise with VCO". As seen in Figure 13, the expected magnetic spectrum is now well above the system noise floor throughout the entire frequency range

(.01 Hz to about 40 Hz). The data taken during the last 4 hours of measurement confirmed this, however, the frequency is still limited to a few Hz because the actual signal strength falls below the sensor sensitivity above 2 to 3 Hz.

All of the system noise measurements were made without the sensor. The sensitivity of the sensor is .005 nT, which is plotted as a dotted line in Figure 13. As is seen, above 10 Hz the expected magnetic spectrum falls below sensor sensitivity. This was also confirmed by the last 4 hours of data. The data showed the coverage to be limited by sensor sensitivity at a few Hz rather than 10 Hz. This is due to the attenuation by sea water, since the "expected magnetic spectrum" shown in Figure 13 is that for the surface of the earth. In sea water the expected spectrum falls off rapidly above 1 Hz (.08 dB/m at 5 Hz).

IV. EXPERIMENTAL RESULTS

A. OBSERVED SPECTRA

The fourteen hours of recorded data were taken at several locations in Monterey Bay at various depths. The spectrum plots are labeled by station numbers corresponding to the list below:

1. STA 1: LAT- 36°43.4'N, LONG 121° 54.5'W
2. STA 2: LAT- 36°54.8'N, LONG 122° 03.0'W
3. STA 3: LAT- 36°52.3'N, LONG 122° 04.7'W
4. STA 4: LAT- 48°51.0'N, LONG 122° 04.7'W
5. STA 5: LAT- 36°47.8'N, LONG 121° 51.4'W
6. STA 6: LAT- 36°49.6'N, LONG 121° 56.3'W
7. STA 7: LAT- 36°52.4'N, LONG 122° 02.3'W

The depth of the water and the date and time of the measurement are recorded on each plot. Each spectrum analysis has the noise floor (excluding sensor noise) of the system used indicated by a dashed line.

The first 5 hours of data (Figures 14 through 18) were recorded using the initial system (without VCO). Consequently, the frequency was limited at the upper end of the band to approximately .1 Hz. After that, the signal approached the noise floor. The second five hours of data (Figures 19 through 23) were recorded using the VCO system. This increased the frequency coverage to approximately 1 Hz. Addition of the 20 dB preamp stage to the VCO was used to record the last four hours of data (Figures 24 through 27). This expanded the frequency coverage out to approximately 3 Hz. The frequency coverage for the last four hours of data was limited by sensor sensitivity, which is shown by a dotted line in Figures 24 through 27.

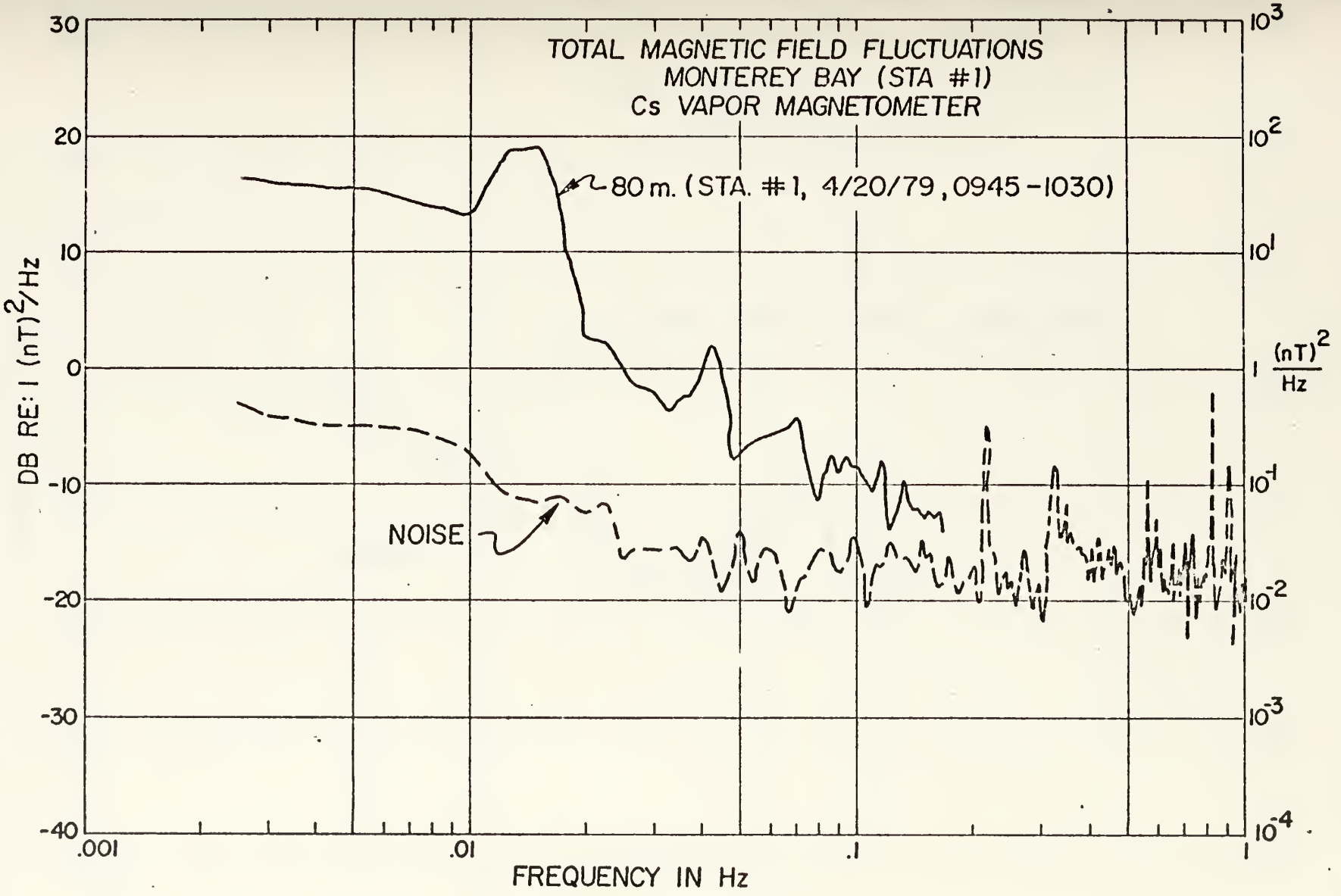
TOTAL MAGNETIC FIELD FLUCTUATIONS
MONTEREY BAY (STA #1)
Cs VAPOR MAGNETOMETER
80 m. (STA. #1, 4/20/79, 0945-1030)
NOISE
DB RE: 1 (nT)²/Hz
(nT)²/Hz
FREQUENCY IN Hz
30
20
10
0
-10
-20
-30
-40
10³
10²
10¹
1
10⁻¹
10⁻²
10⁻³
10⁻⁴
.001
.01
.1
1

Figure 14

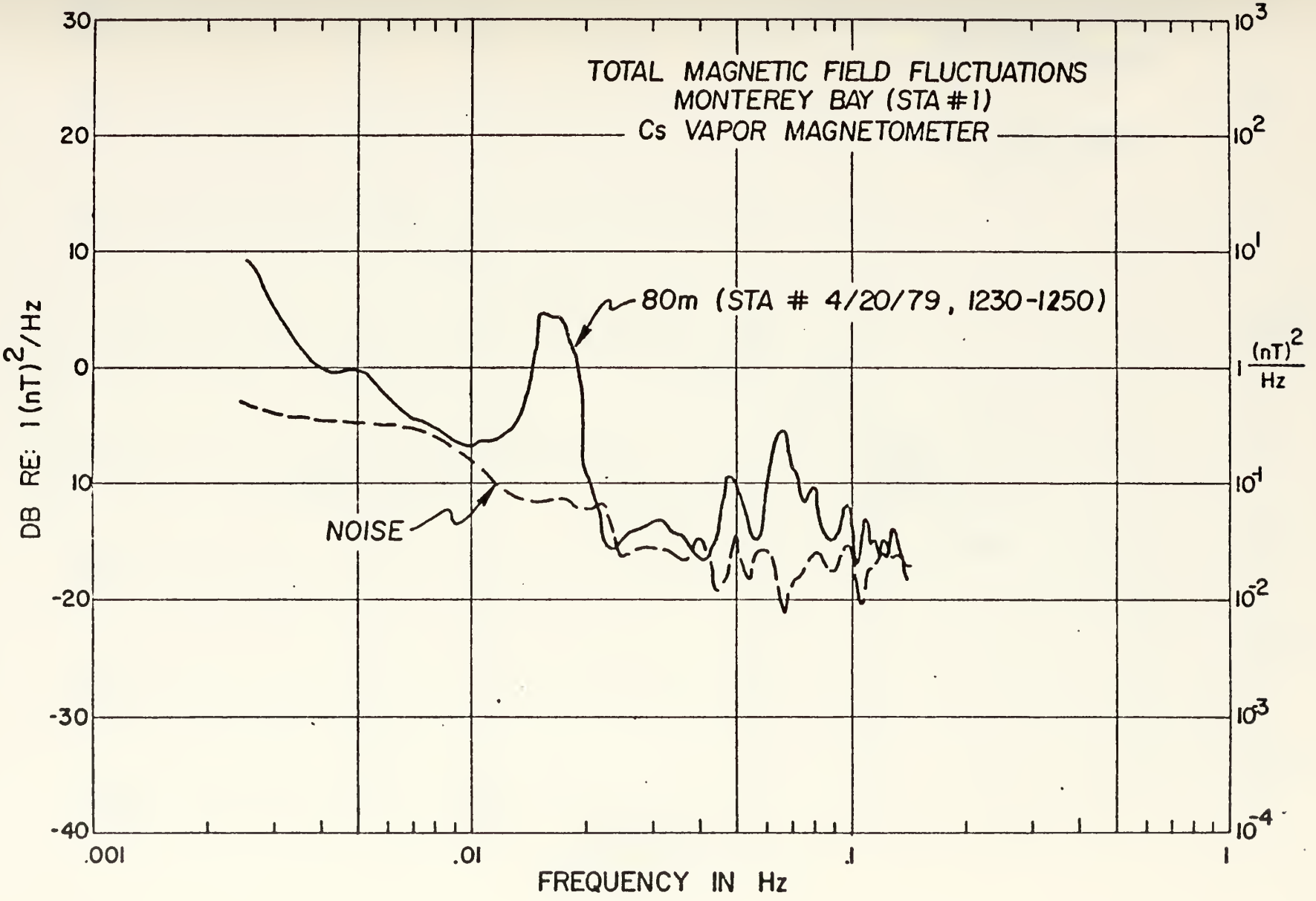
TOTAL MAGNETIC FIELD FLUCTUATIONS
MONTEREY BAY (STA #1)
Cs VAPOR MAGNETOMETER
80m (STA # 4/20/79, 1230-1250)
NOISE
DB RE: 1 (nT)²/Hz
FREQUENCY IN Hz
1 (nT)²/Hz
30
20
10
0
10
-20
-30
-40
.001
.01
.1
1
10³
10²
10¹
10⁻¹
10⁻²
10⁻³
10⁻⁴

Figure 15

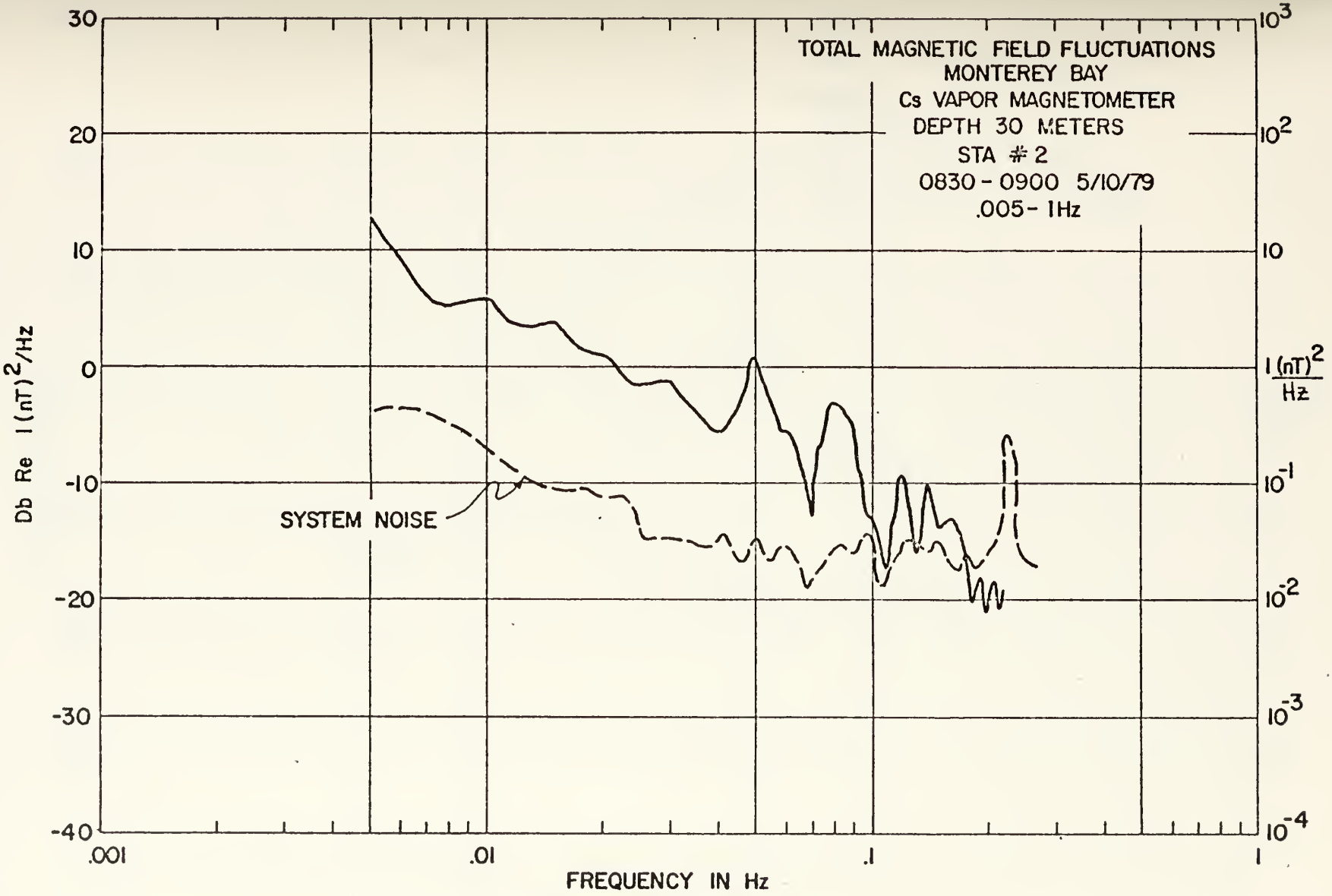
TOTAL MAGNETIC FIELD FLUCTUATIONS
MONTEREY BAY
Cs VAPOR MAGNETOMETER
DEPTH 30 METERS
STA # 2
0830 - 0900 5/10/79
.005 - 1Hz
SYSTEM NOISE
Db Re 1 (nT)²/Hz
1 (nT)²/Hz
FREQUENCY IN Hz
30
20
10
0
-10
-20
-30
-40
10³
10²
10
1
10⁻¹
10⁻²
10⁻³
10⁻⁴
.001
.01
.1
1

Figure 16

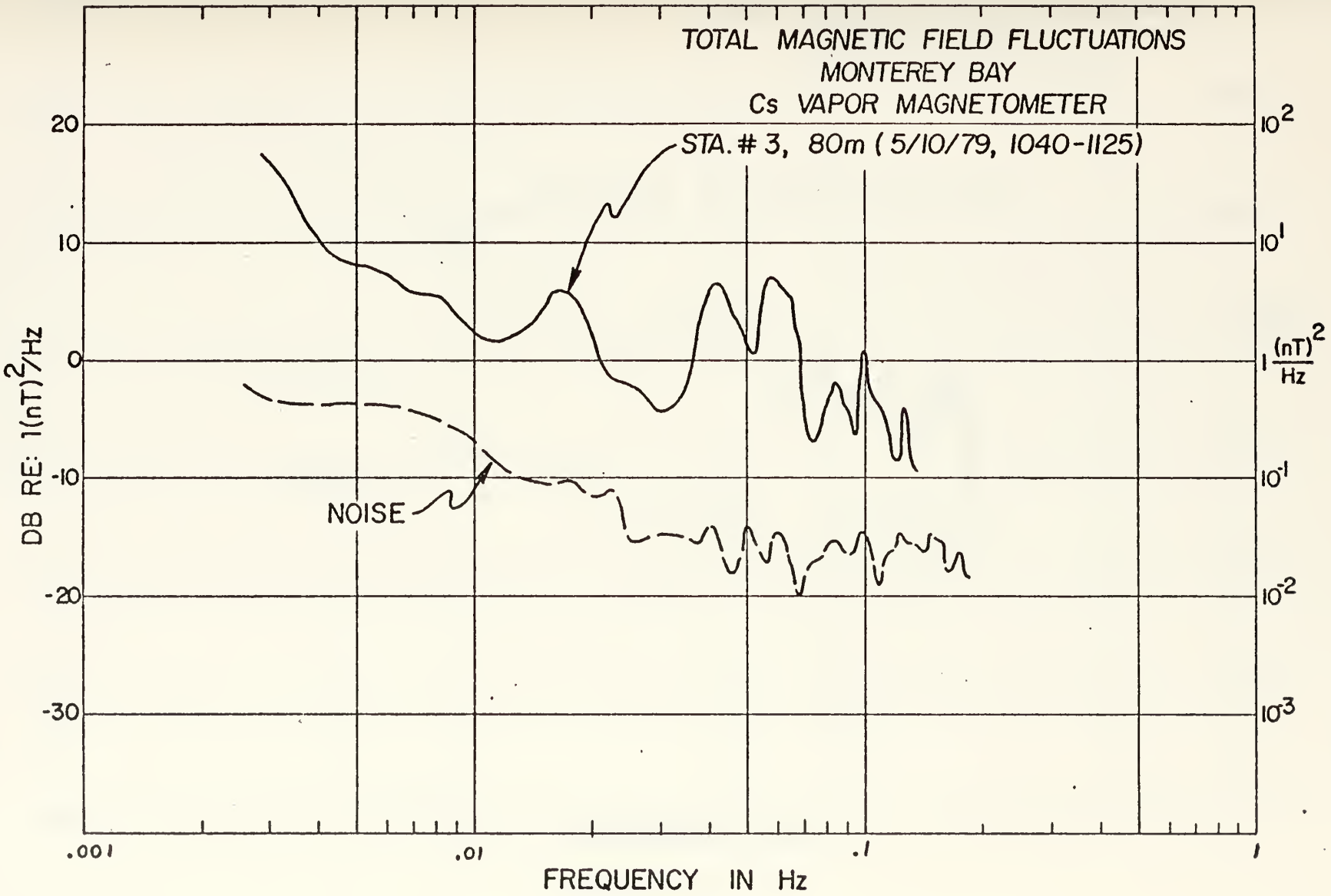
TOTAL MAGNETIC FIELD FLUCTUATIONS
MONTEREY BAY
Cs VAPOR MAGNETOMETER
STA. # 3, 80m (5/10/79, 1040-1125)
NOISE
DB RE: 1(nT)²/Hz
20
10
0
-10
-20
-30
10²
10¹
1 (nT)²/Hz
10⁻¹
10⁻²
10⁻³
.001
.01
.1
1
FREQUENCY IN Hz

Figure 17

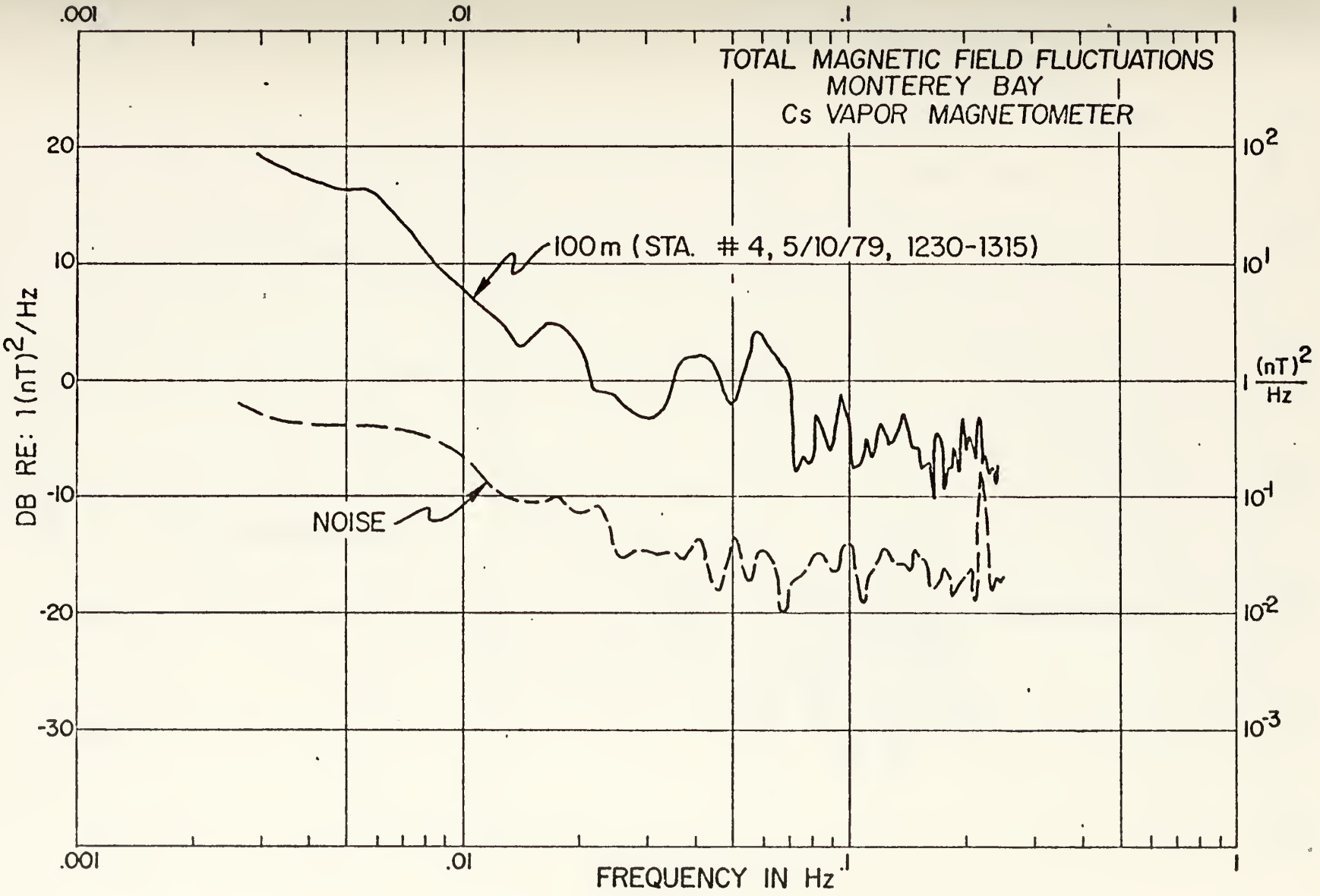
TOTAL MAGNETIC FIELD FLUCTUATIONS
MONTEREY BAY
Cs VAPOR MAGNETOMETER
100 m (STA. # 4, 5/10/79, 1230-1315)
NOISE
DB RE: 1(nT)²/Hz
FREQUENCY IN Hz
.001
.01
.1
1
20
10
0
-10
-20
-30
10²
10¹
1
10⁻¹
10⁻²
10⁻³
(nT)²/Hz

Figure 18

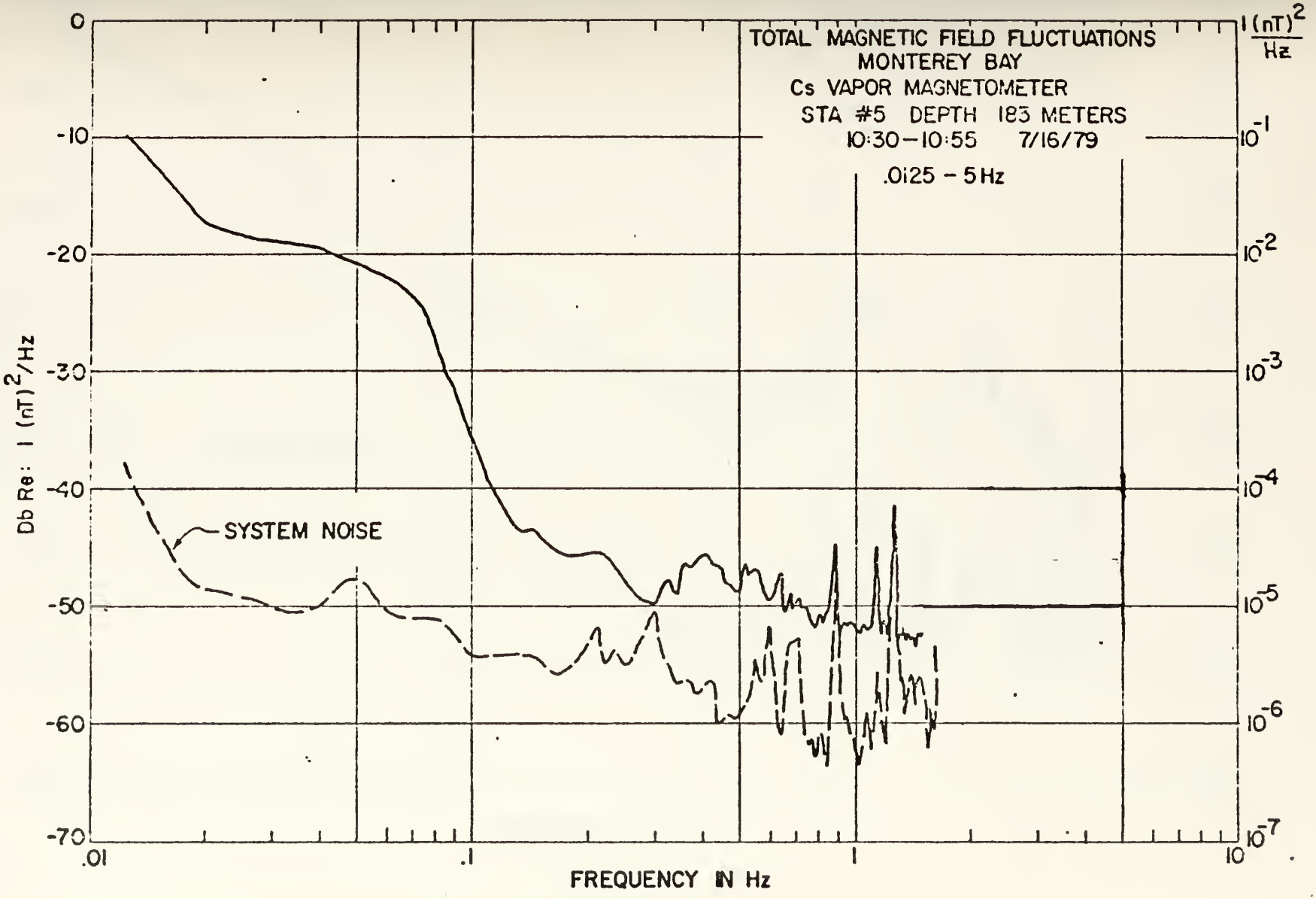
TOTAL MAGNETIC FIELD FLUCTUATIONS
MONTEREY BAY
Cs VAPOR MAGNETOMETER
STA #5 DEPTH 183 METERS
10:30–10:55 7/16/79
.0125 – 5 Hz
SYSTEM NOISE
Db Re: 1 (nT)²/Hz
1 (nT)²/Hz
FREQUENCY IN Hz
0
-10
-20
-30
-40
-50
-60
-70
10⁻¹
10⁻²
10⁻³
10⁻⁴
10⁻⁵
10⁻⁶
10⁻⁷
.01
.1
1
10

Figure 19

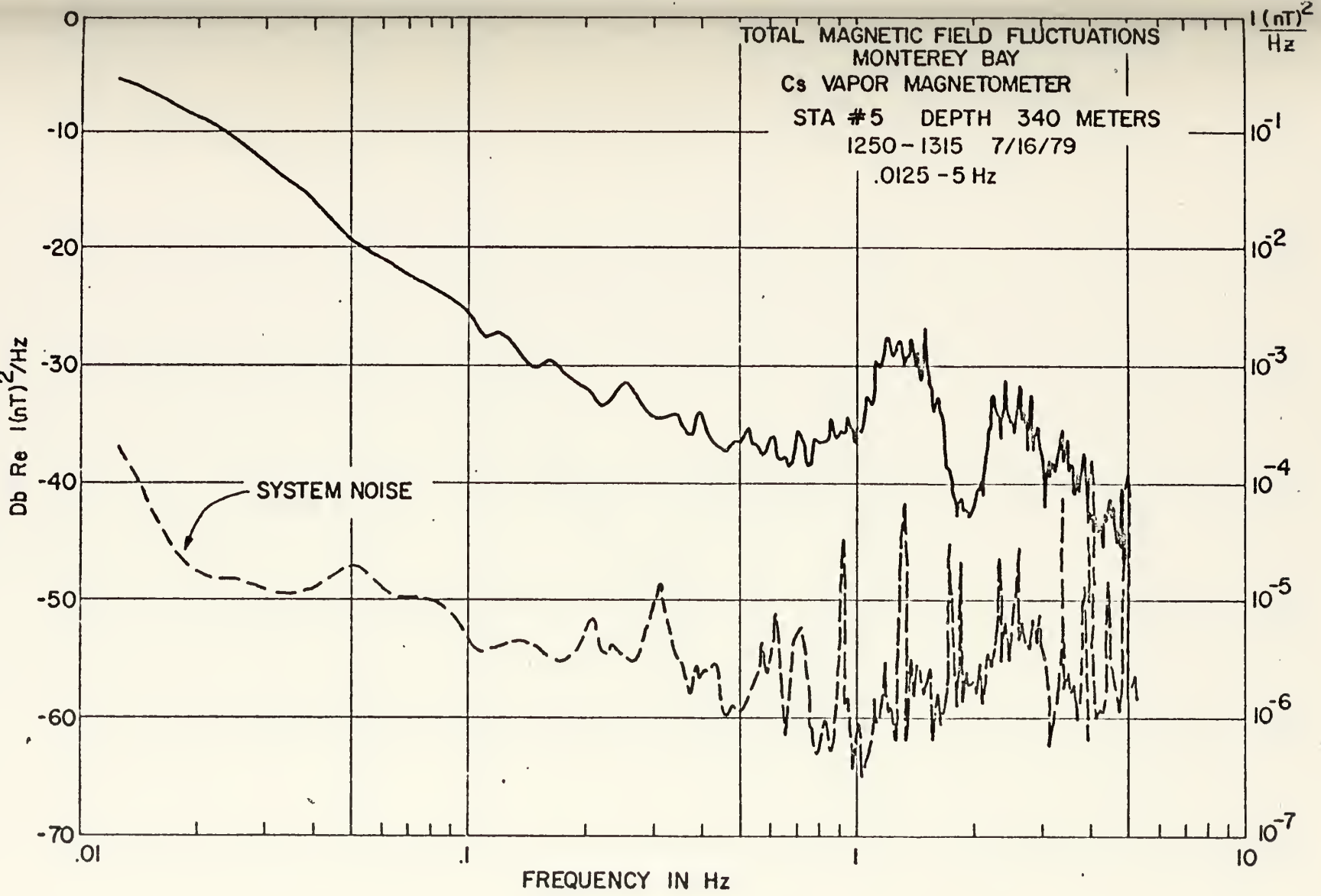
TOTAL MAGNETIC FIELD FLUCTUATIONS
MONTEREY BAY
Cs VAPOR MAGNETOMETER
STA #5 DEPTH 340 METERS
1250 - 1315 7/16/79
.0125 - 5 Hz
SYSTEM NOISE
Db Re 1(nT)²/Hz
1 (nT)²/Hz
0
-10
-20
-30
-40
-50
-60
-70
10⁻¹
10⁻²
10⁻³
10⁻⁴
10⁻⁵
10⁻⁶
10⁻⁷
.01
.1
1
10
FREQUENCY IN Hz

Figure 20

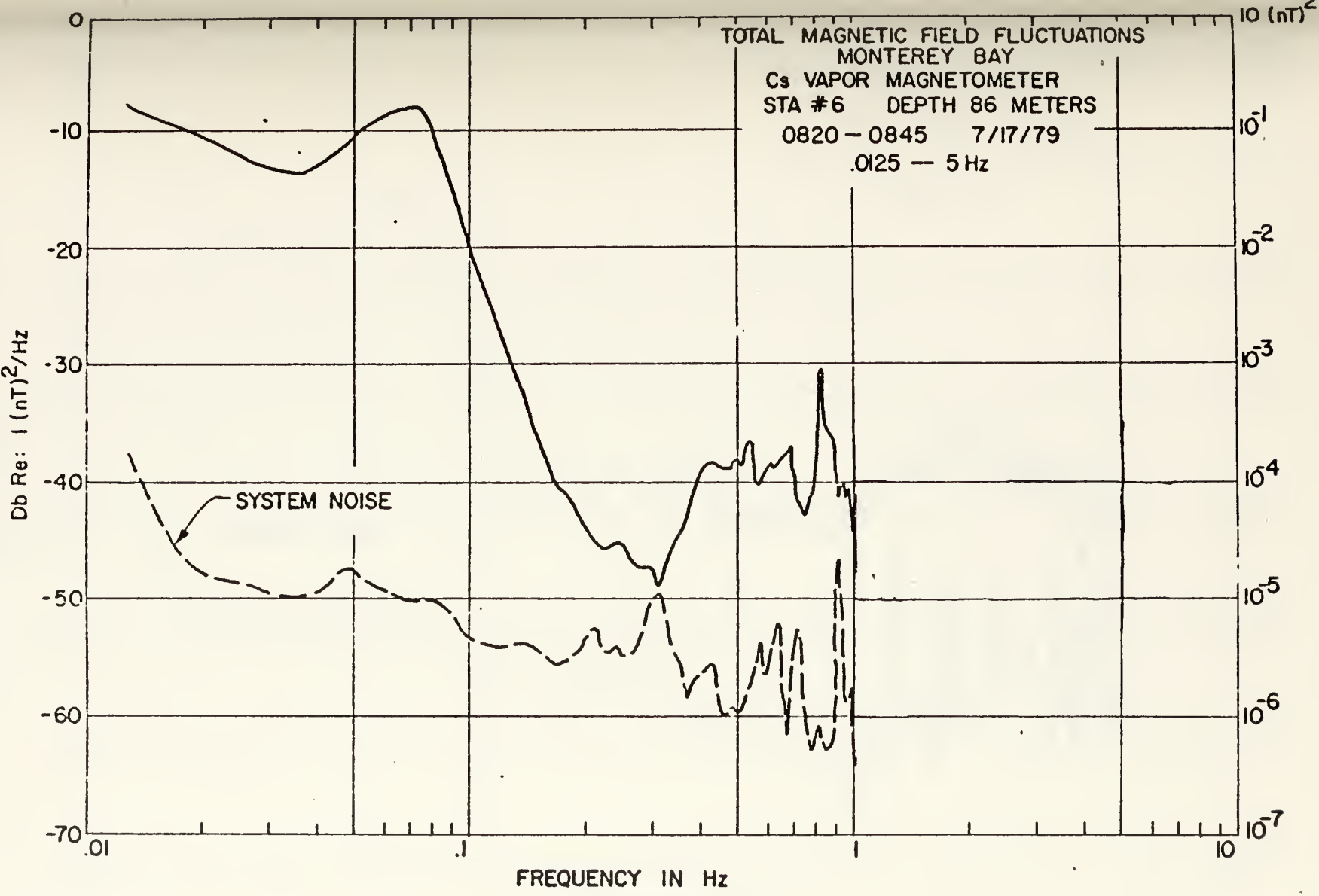
TOTAL MAGNETIC FIELD FLUCTUATIONS
MONTEREY BAY
Cs VAPOR MAGNETOMETER
STA #6 DEPTH 86 METERS
0820 – 0845 7/17/79
.0125 — 5 Hz
SYSTEM NOISE
Db Re: 1 (nT)²/Hz
10 (nT)²
0
-10
-20
-30
-40
-50
-60
-70
10⁻¹
10⁻²
10⁻³
10⁻⁴
10⁻⁵
10⁻⁶
10⁻⁷
.01
.1
1
10
FREQUENCY IN Hz

Figure 21

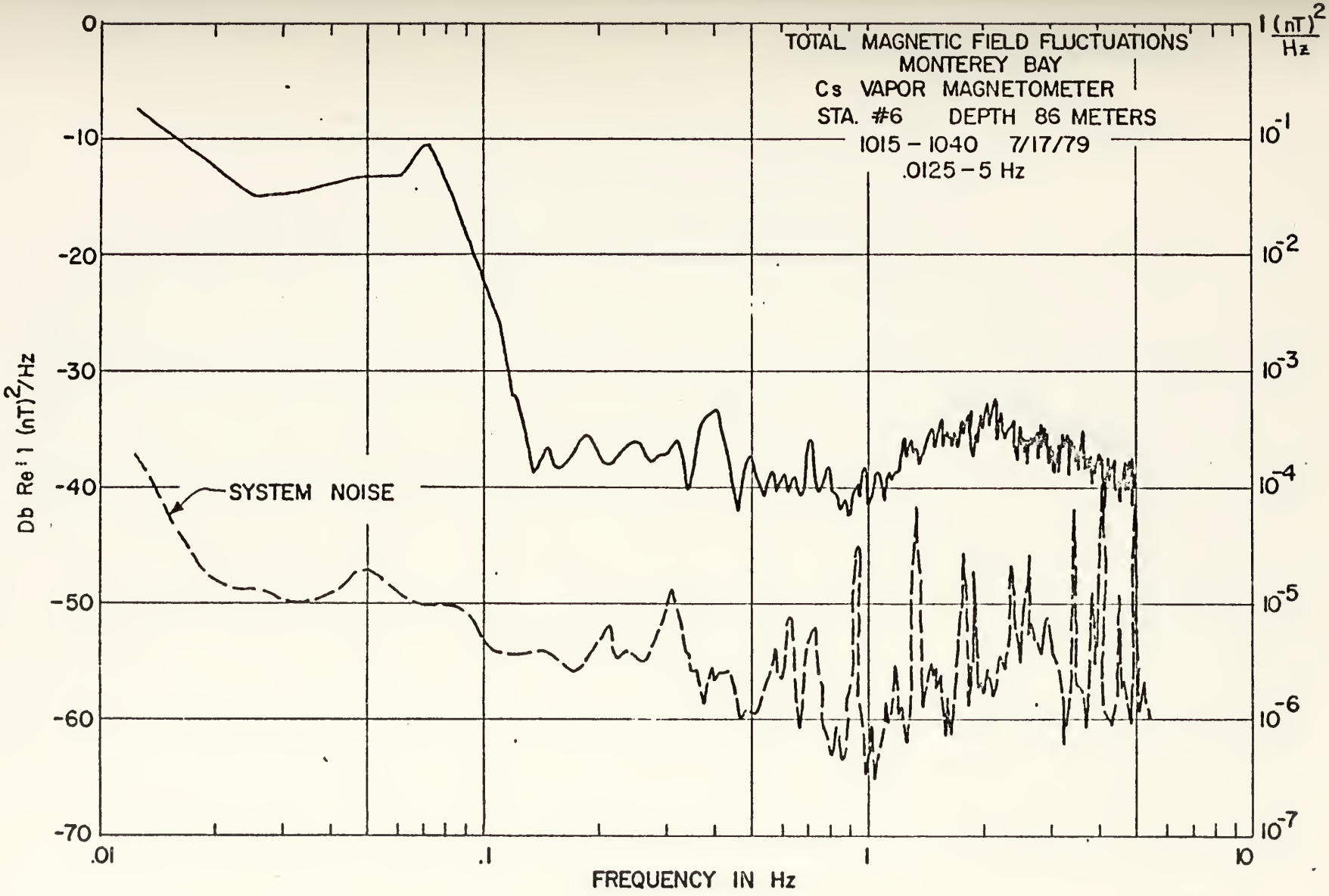
TOTAL MAGNETIC FIELD FLUCTUATIONS
MONTEREY BAY
Cs VAPOR MAGNETOMETER
STA. #6 DEPTH 86 METERS
1015 – 1040 7/17/79
.0125 – 5 Hz
SYSTEM NOISE
Db Re 1 (nT)²/Hz
1 (nT)²/Hz
0
-10
-20
-30
-40
-50
-60
-70
10⁻¹
10⁻²
10⁻³
10⁻⁴
10⁻⁵
10⁻⁶
10⁻⁷
.01
.1
1
10
FREQUENCY IN Hz

Figure 22

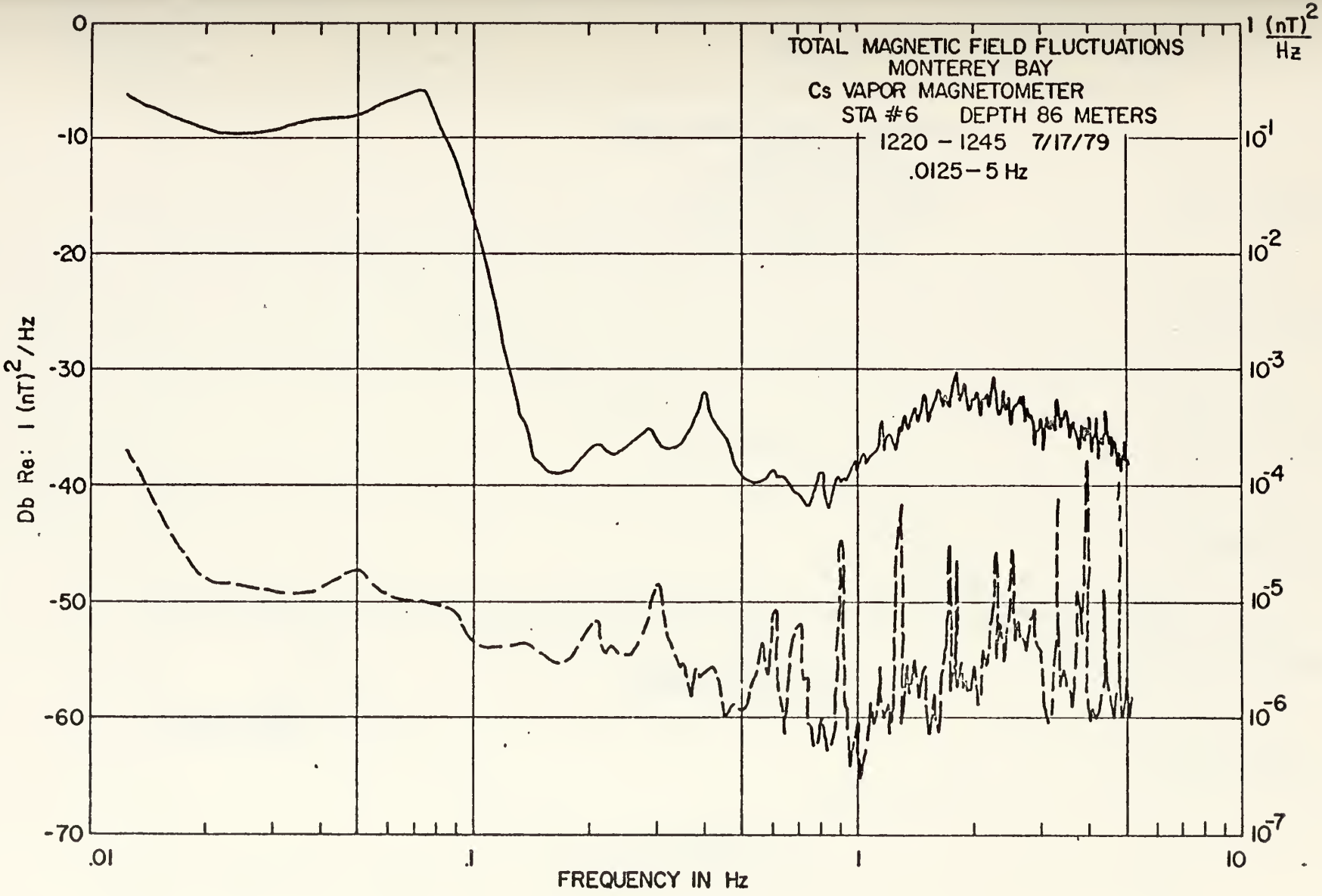
TOTAL MAGNETIC FIELD FLUCTUATIONS
MONTEREY BAY
Cs VAPOR MAGNETOMETER
STA #6 DEPTH 86 METERS
1220 – 1245 7/17/79
.0125 – 5 Hz
Db Re: 1 (nT)²/Hz
1 (nT)²/Hz
0
-10
-20
-30
-40
-50
-60
-70
10⁻¹
10⁻²
10⁻³
10⁻⁴
10⁻⁵
10⁻⁶
10⁻⁷
.01
.1
1
10
FREQUENCY IN Hz

Figure 23

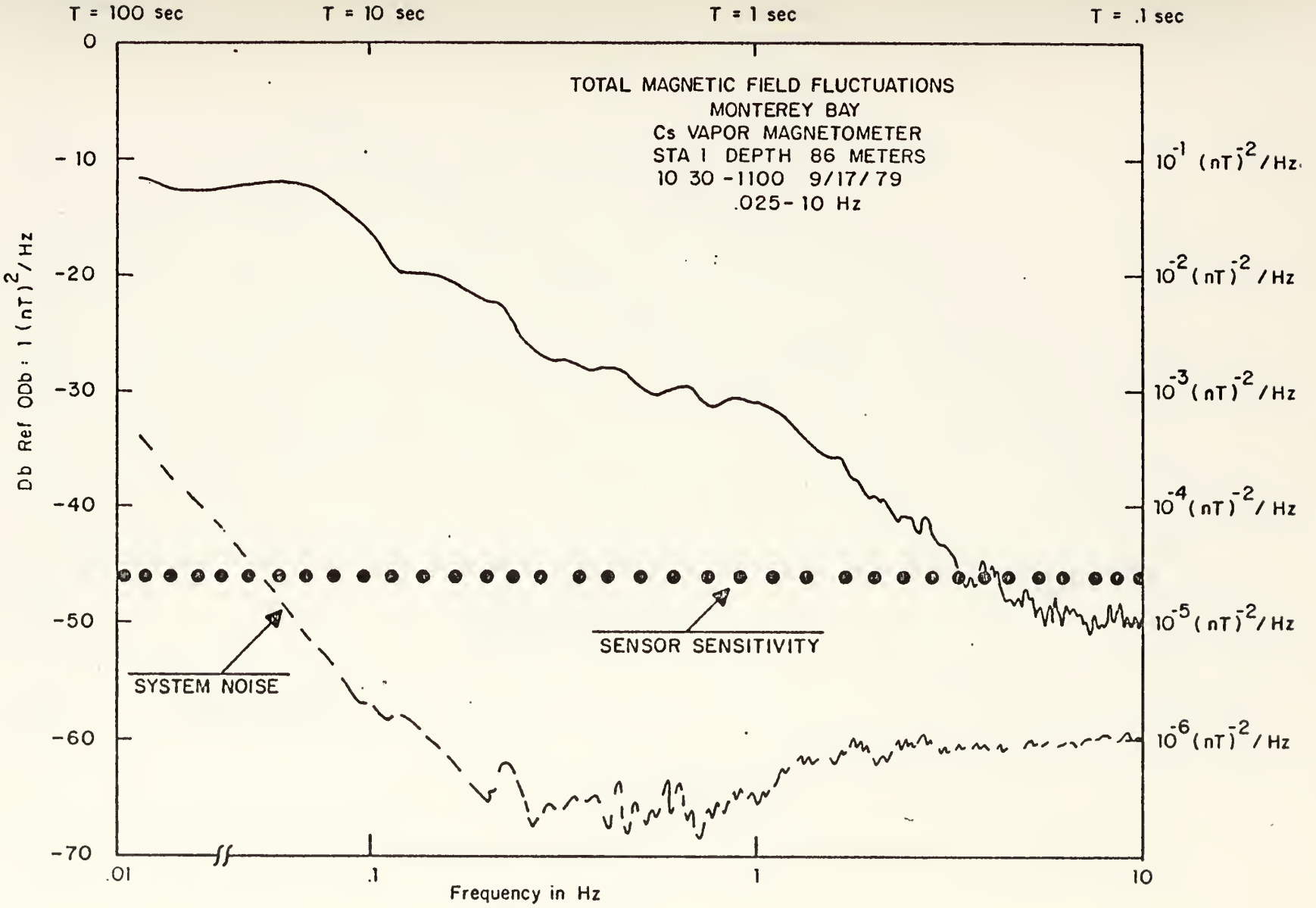
T = 100 sec
T = 10 sec
T = 1 sec
T = .1 sec
TOTAL MAGNETIC FIELD FLUCTUATIONS
MONTEREY BAY
Cs VAPOR MAGNETOMETER
STA 1 DEPTH 86 METERS
10 30 -1100 9/17/79
.025- 10 Hz
Db Ref ODb = 1 (nT)^2/Hz
0
-10
-20
-30
-40
-50
-60
-70
10^{-1} (nT)$^{-2}$/Hz
10^{-2} (nT)$^{-2}$/Hz
10^{-3} (nT)$^{-2}$/Hz
10^{-4} (nT)$^{-2}$/Hz
10^{-5} (nT)$^{-2}$/Hz
10^{-6} (nT)$^{-2}$/Hz
SYSTEM NOISE
SENSOR SENSITIVITY
.01
.1
1
10
Frequency in Hz

Figure 24.

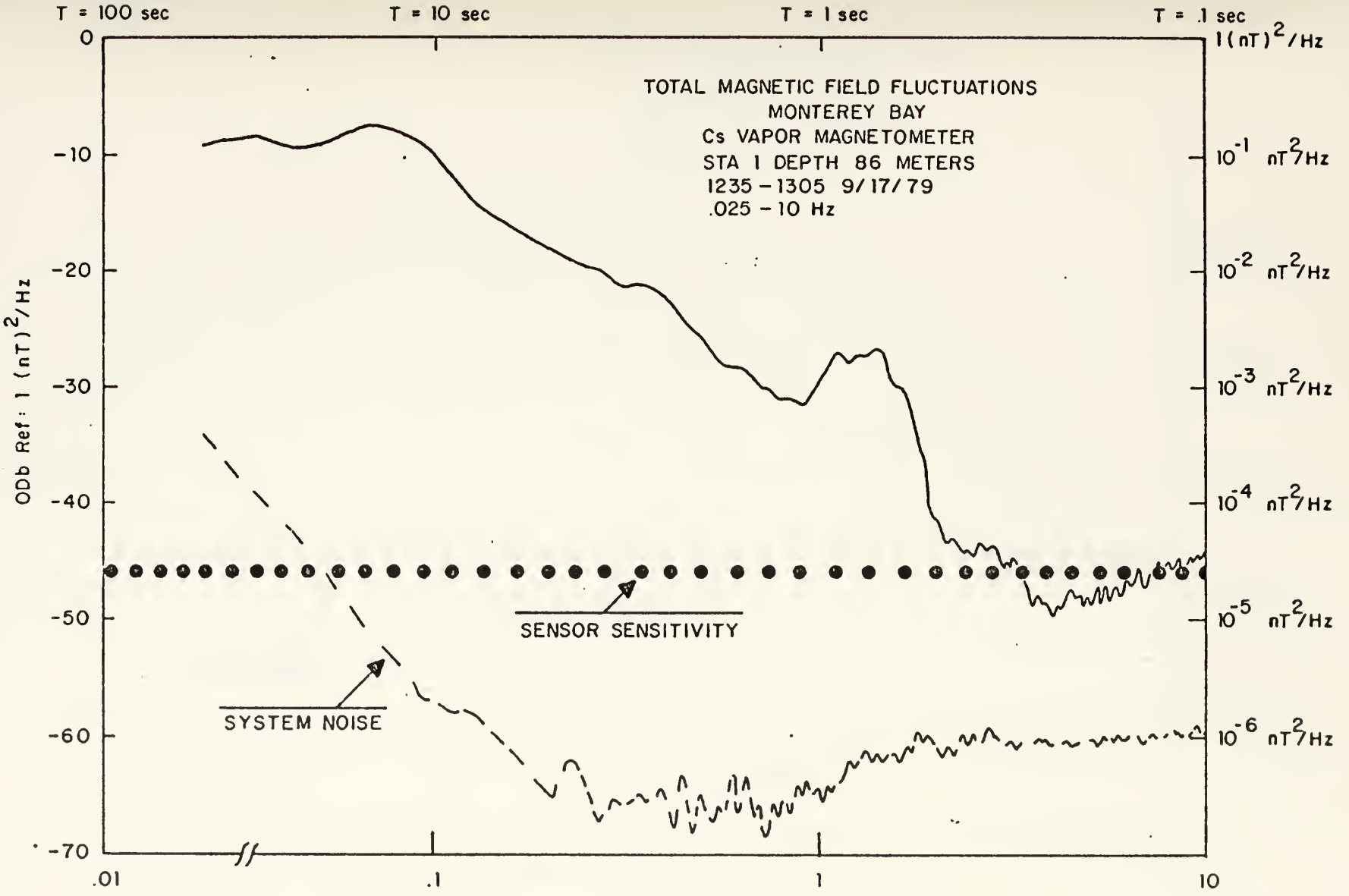
T = 100 sec
T = 10 sec
T = 1 sec
T = .1 sec
1 (nT)²/Hz
TOTAL MAGNETIC FIELD FLUCTUATIONS
MONTEREY BAY
Cs VAPOR MAGNETOMETER
STA 1 DEPTH 86 METERS
1235 – 1305 9/17/79
.025 – 10 Hz
0
-10
-20
-30
-40
-50
-60
-70
ODb Ref: 1 (nT)²/Hz
10⁻¹ nT²/Hz
10⁻² nT²/Hz
10⁻³ nT²/Hz
10⁻⁴ nT²/Hz
10⁻⁵ nT²/Hz
10⁻⁶ nT²/Hz
SENSOR SENSITIVITY
SYSTEM NOISE
.01
.1
1
10
Frequency in Hz

Figure 25

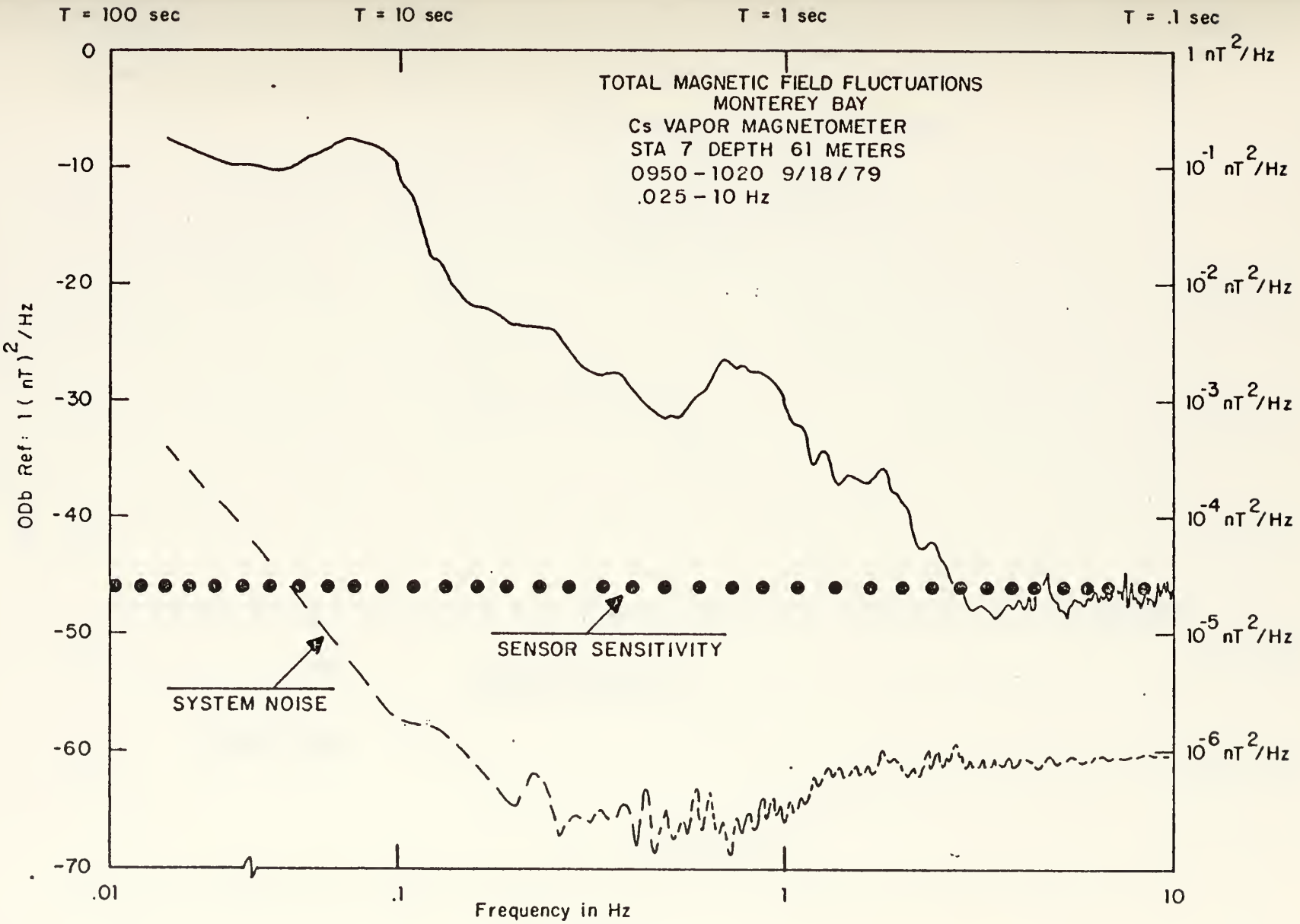
T = 100 sec
T = 10 sec
T = 1 sec
T = .1 sec
TOTAL MAGNETIC FIELD FLUCTUATIONS
MONTEREY BAY
Cs VAPOR MAGNETOMETER
STA 7 DEPTH 61 METERS
0950 - 1020 9/18/79
.025 - 10 Hz
SENSOR SENSITIVITY
SYSTEM NOISE
0
-10
-20
-30
-40
-50
-60
-70
ODb Ref: 1 (nT)^2/Hz
1 nT^2/Hz
10^{-1} nT^2/Hz
10^{-2} nT^2/Hz
10^{-3} nT^2/Hz
10^{-4} nT^2/Hz
10^{-5} nT^2/Hz
10^{-6} nT^2/Hz
.01
.1
1
10
Frequency in Hz

Figure 26.

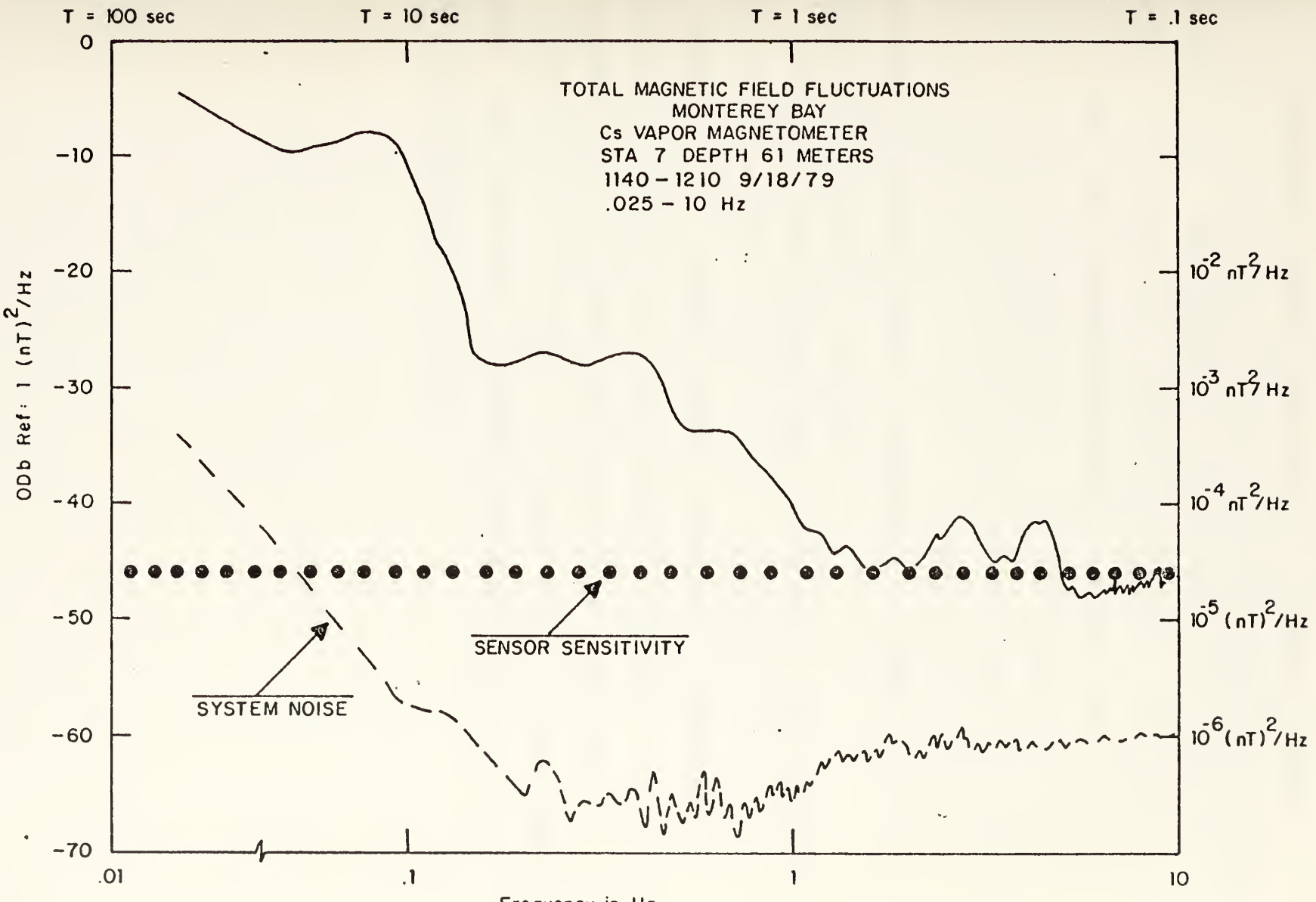
T = 100 sec
T = 10 sec
T = 1 sec
T = .1 sec
TOTAL MAGNETIC FIELD FLUCTUATIONS
MONTEREY BAY
Cs VAPOR MAGNETOMETER
STA 7 DEPTH 61 METERS
1140 - 1210 9/18/79
.025 - 10 Hz
0
-10
-20
-30
-40
-50
-60
-70
ODb Ref: 1 (nT)²/Hz
10⁻² nT²/Hz
10⁻³ nT²/Hz
10⁻⁴ nT²/Hz
10⁻⁵ (nT)²/Hz
10⁻⁶ (nT)²/Hz
SENSOR SENSITIVITY
SYSTEM NOISE
.01
.1
1
10
Frequency in Hz

Figure 27

B. OCEAN WAVE SPECTRA COMPARISON

A comparison between geomagnetic variations recorded on the ocean floor and the surface wave height spectrum is shown in Figure 28. The geomagnetic sensor was in 120 feet of water on the ocean floor (36°55'N, 122°03'W). The "Wave Rider" buoy was located approximately one-half mile laterally from the position of the sensor. Due to the spacial difference in locations, the correlation between wave height data and geomagnetic data is limited. In future measurements to correlate ocean wave data, the geomagnetic sensor will be placed directly under the buoy.

During the measurement shown in Figure 28, the Research Ship Acania passed over the sensor. Figure 29 shows the time plot of the magnetic anomaly produced by the vessel. As is seen in Figure 29, the time plot is similar to that expected for an extremely large MAD signal. The Acania is a metal ship and could have interfered with the measurements. During data recording, the Acania stood off approximately one mile from sensor location.

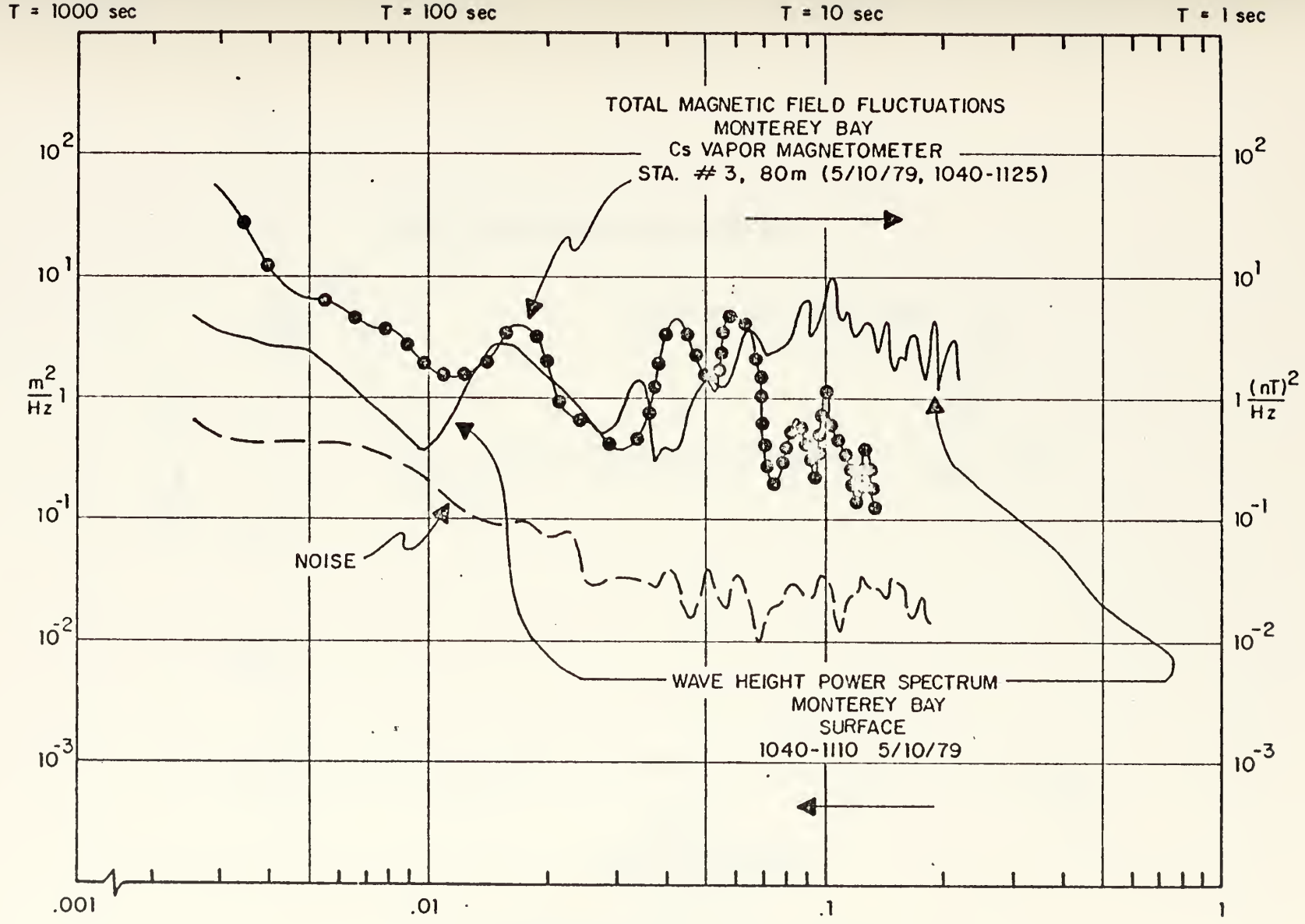
T = 1000 sec
T = 100 sec
T = 10 sec
T = 1 sec
TOTAL MAGNETIC FIELD FLUCTUATIONS
MONTEREY BAY
Cs VAPOR MAGNETOMETER
STA. # 3, 80m (5/10/79, 1040-1125)
NOISE
WAVE HEIGHT POWER SPECTRUM
MONTEREY BAY
SURFACE
1040-1110 5/10/79
10^2
10^1
1
10^{-1}
10^{-2}
10^{-3}
$\frac{m^2}{Hz}$
$\frac{(nT)^2}{Hz}$
.001
.01
.1
1
Frequency In Hz

Figure 28

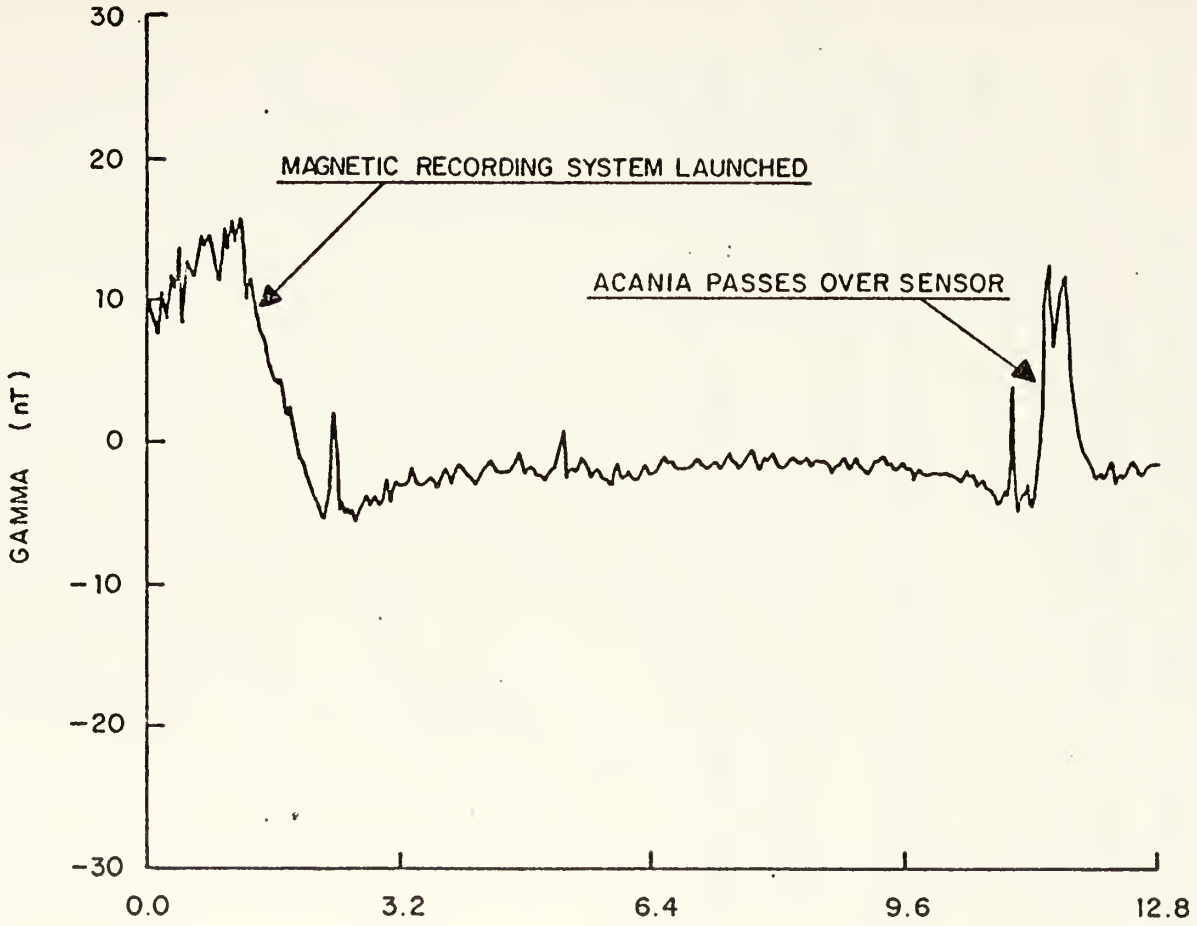

Figure 29

Research Ship Acania Magnetic Anonomly Signal

C. SPECTRA COMPILATION

For ease of discussion, the 14 hours of data is combined on three plots. Figure 30 is a plot of the first five hours of data. In Figure 31, the second five hours of data is given. And finally, Figure 32 is a plot of the last four hours of data. They are grouped this way for two reasons:

1. According to recording system used: preliminary system, system with VCO, and VCO system with additional 20 dB preamp respectively.

2. Geomagnetic activity and weather conditions were similar for the above groupings.

A description of the environmental conditions and the salient features of the spectra is given in the next section.

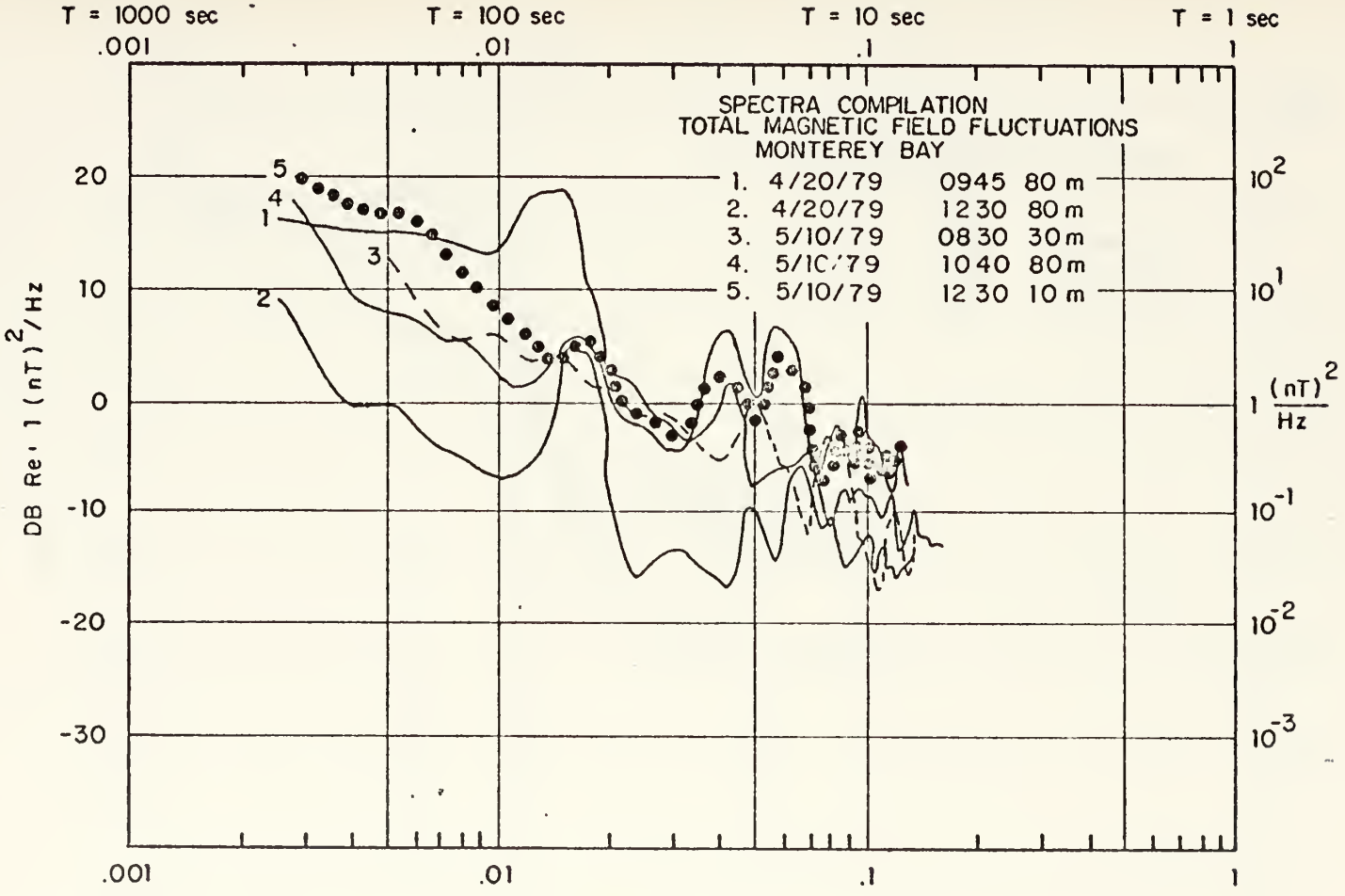
T = 1000 sec
T = 100 sec
T = 10 sec
T = 1 sec
.001
.01
.1
1
SPECTRA COMPILATION
TOTAL MAGNETIC FIELD FLUCTUATIONS
MONTEREY BAY
1. 4/20/79 0945 80 m
2. 4/20/79 1230 80 m
3. 5/10/79 0830 30 m
4. 5/10/79 1040 80 m
5. 5/10/79 1230 10 m
20
10
0
-10
-20
-30
DB Re 1 (nT)²/Hz
10²
10¹
1 (nT)²/Hz
10⁻¹
10⁻²
10⁻³
Frequency in Hz
Figure 30

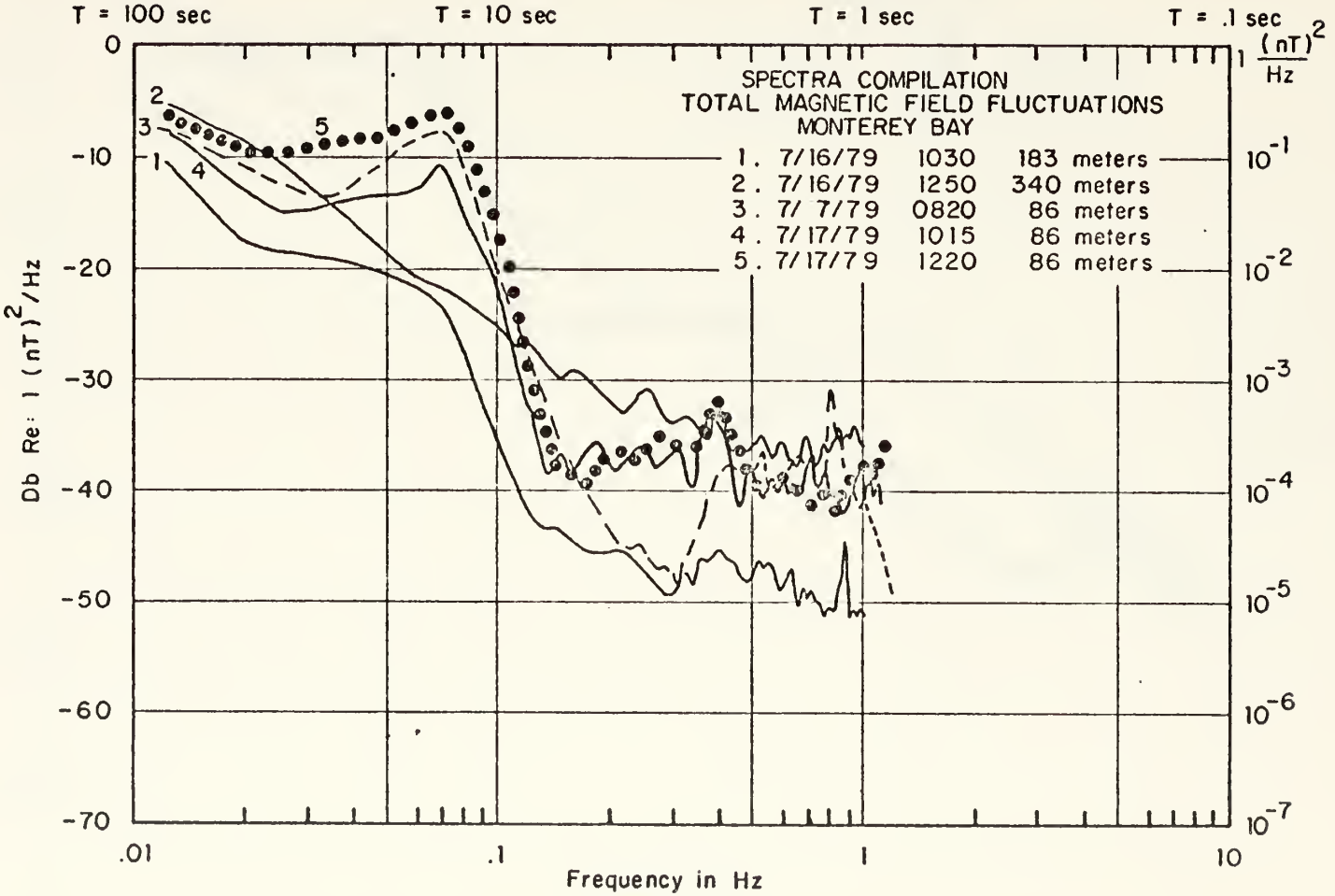
T = 100 sec
T = 10 sec
T = 1 sec
T = .1 sec
SPECTRA COMPILATION
TOTAL MAGNETIC FIELD FLUCTUATIONS
MONTEREY BAY
1. 7/16/79 1030 183 meters
2. 7/16/79 1250 340 meters
3. 7/ 7/79 0820 86 meters
4. 7/17/79 1015 86 meters
5. 7/17/79 1220 86 meters
Db Re: 1 (nT)²/Hz
0
-10
-20
-30
-40
-50
-60
-70
1 (nT)²/Hz
10⁻¹
10⁻²
10⁻³
10⁻⁴
10⁻⁵
10⁻⁶
10⁻⁷
.01
.1
1
10
Frequency in Hz

Figure 31.

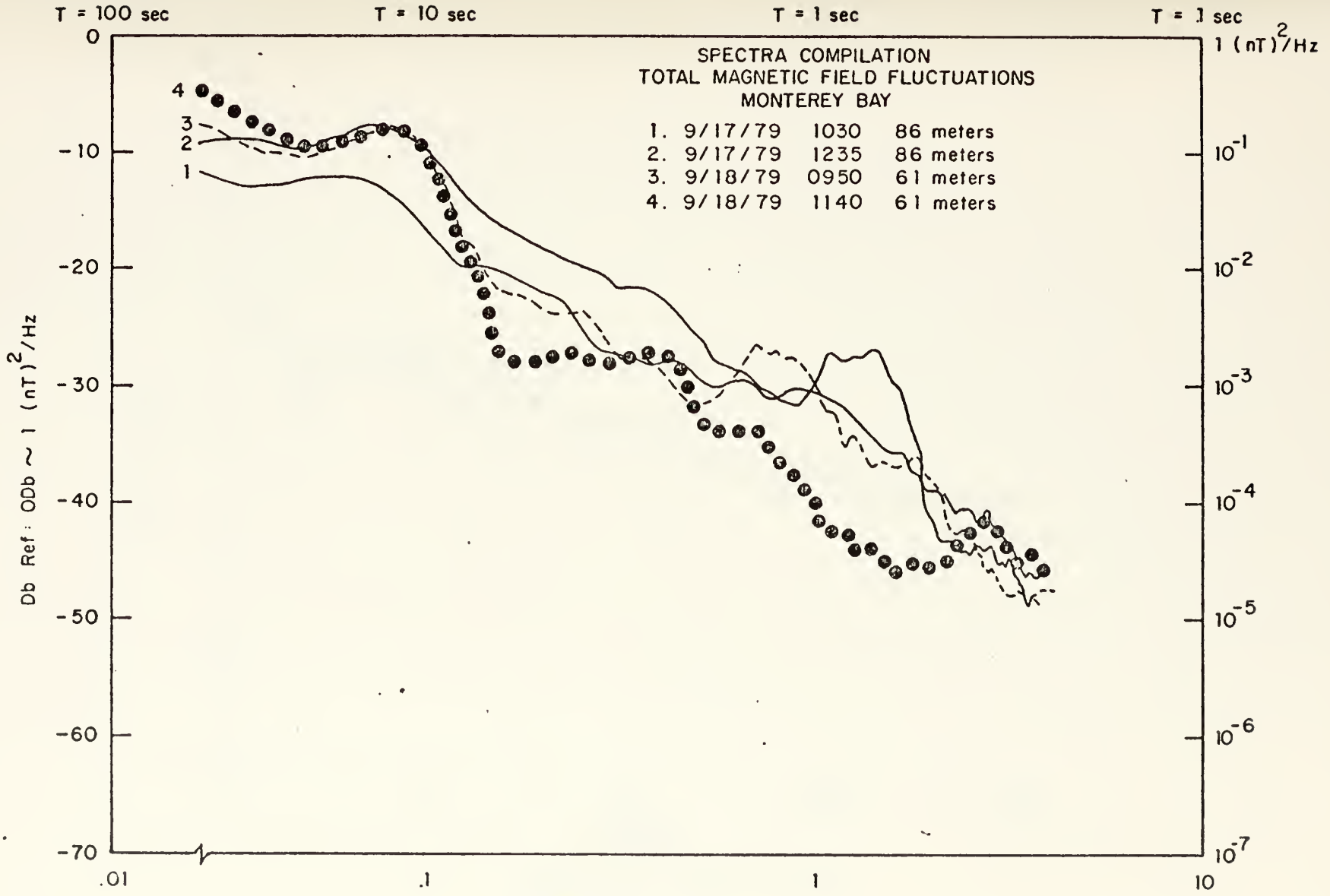
T = 100 sec
T = 10 sec
T = 1 sec
T = .1 sec
SPECTRA COMPILATION
TOTAL MAGNETIC FIELD FLUCTUATIONS
MONTEREY BAY
1. 9/17/79 1030 86 meters
2. 9/17/79 1235 86 meters
3. 9/18/79 0950 61 meters
4. 9/18/79 1140 61 meters
Db Ref: 0Db ~ 1 (nT)²/Hz
1 (nT)²/Hz
0
-10
-20
-30
-40
-50
-60
-70
10⁻¹
10⁻²
10⁻³
10⁻⁴
10⁻⁵
10⁻⁶
10⁻⁷
.01
.1
1
10
Frequency in Hz

Figure 32

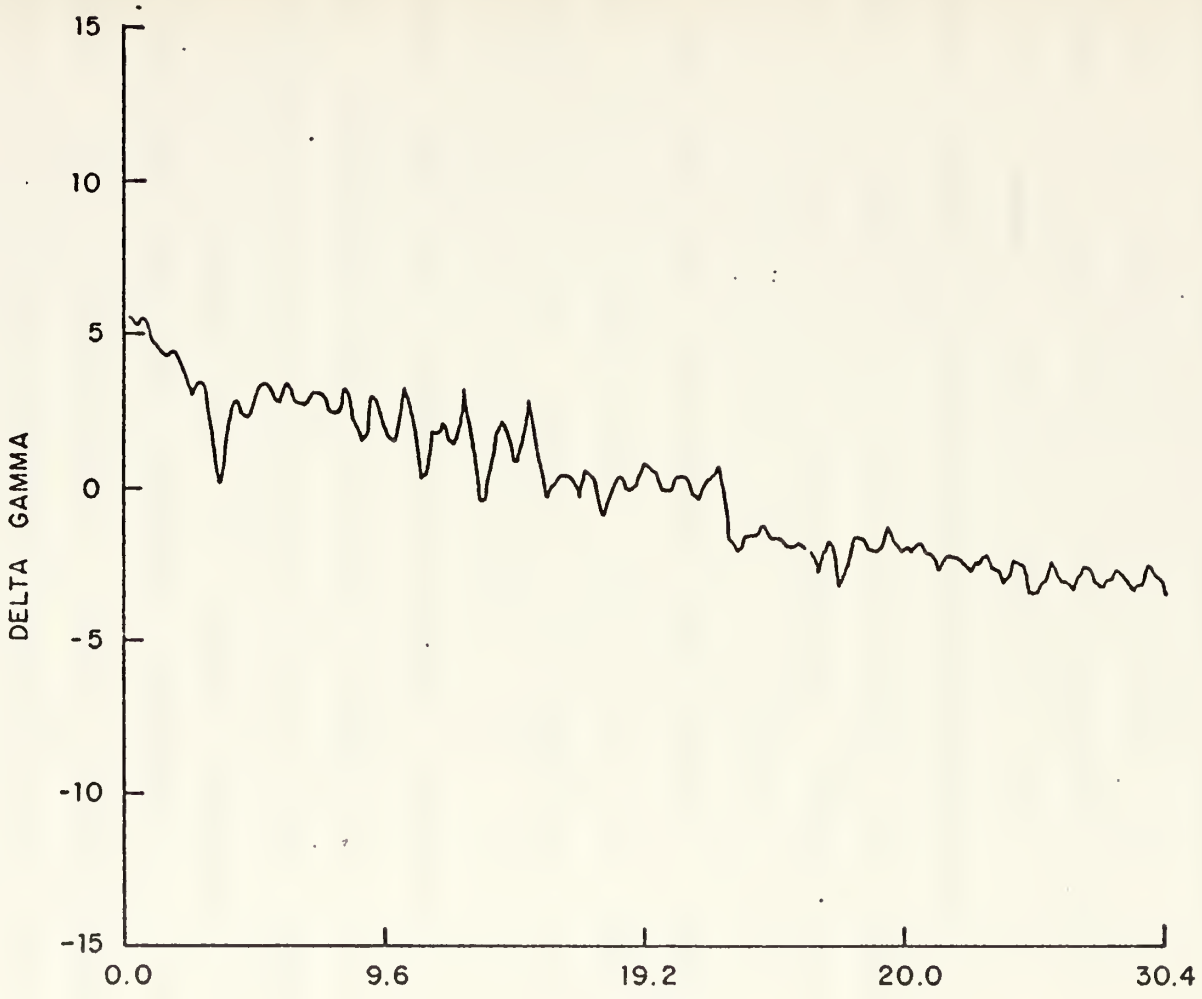

Figure 33.

Monterey Bay 4/20/79 0945

D. DISCUSSION OF DATA

The following discussion will be referenced to the last five figures (Figures 28 through 32).

1. Figure 28 - Surface Ocean Wave and Magnetic Variation Comparison

The depth of the ocean at the sensors location was approximately 260 feet while the depth of the water at the Wave Rider buoy location was about 200 feet. Also there was approximately a one-half mile lateral separation between the buoy and the sensor. The most predominant wave period observed visually during the measurements was around T=10 seconds. In Figure 28 the best correlation of the frequency maxima occurs at .1 Hz (10 second period). Referring to Figure 4, it can be seen that for a 10 second period of one meter amplitude wave, the induced field should be approximately .35nT at 80 meters depth. At f=.1 Hz, the ocean wave magnitude was 10 m^2/Hz. Therefore, the magnitude of the ocean wave was about 3.2 meters/$Hz^{\frac{1}{2}}$ at .1 Hz. Multiplying 3.2 times .35nT gives an expected magnetic variation of 1.1nT. The measured value (as seen in Figure 28) is 1.1nT. The frequency correlation was not as good at other frequencies. This is probably due to the spatial separation of sensor and buoy along with the depth difference at the two locations. Due to the proximity of land in these measurements, relatively small distances in location can make a big difference in wave spectra due to land shadowing and other shore effects.

2. Figure 29 - Magnetic Anomaly Signal of the Acania passing over the sensor.

In order to determine the effect of the research ship on the measurements, it passed over the sensor while a recording was being conducted. The depth of the sensor at the time of the recording was 30 meters. As is seen in Figure 29, a 15 nT change in magnetic field intensity occurred as the research ship passed overhead. To prevent interference with the geomagnetic measurements, after launching the sensor/recording system, the research ship stood off approximately one mile from the sensor location during measurements.

3. Figure 30 - 4/20/79 and 5/10/79 Data Compilation

This data was recorded with the preliminary system. Consequently, frequency coverage was good only to about .1 Hz. The seas were rough during these five hours of measurements, with winds in excess of 15 knots. The Fredricksburg geomagnetic k indices were 2+ or less during all five hours of measurement (geomagnetically-very quiet). There are several features worth noting on the plot. First, the overall spectrum levels are those expected (see Figure 1). The predominant swell that was observed was around a period of 10 to 15 seconds. As can be seen in Figure 30, predominant peaks are observed from about .05 to .1 Hz (T=20 sec to T=10 sec). An interesting feature observed on the plots is the peak at .015 Hz. This corresponds to a period of about 67 seconds. It is believed that this is from pc 4 micropulsations or from ocean wave grouping whose periods typically vary between 45 sec. to 180 sec.. Figure 33 is a

time plot of the geomagnetic data recorded corresponding to curve 1 in Figure 31. The one minute cyclic nature of the time plot is evident.

4. Figure 31 - 7/16/79 and 7/17/79 Data Compilation

This data was recorded with the VCO system (without 20 dB pre-amp). The frequency coverage is good to about 1 Hz. The seas were moderate and the wind was about 10 knots throughout the five hours of measurement. The Fredricksburg geomagnetic k indices were 3+ or less during the five hours recording (quiet geomagnetically). Two features worth noting are the peaks around .08 Hz and around .4 Hz (T=12.5 seconds and T=2.5 seconds respectively). The 12.5 second period corresponds to the ocean swell period observed visually during the measurements. The 2.5 second period corresponds to wind driven waves on the ocean surface, again visually observed. In comparing curves 1 and 3 (183 meters depth and 86 meters depth), it is noted that the .08 Hz peak is attenuated by approximately 10 dB in the deeper ocean floor case. This is consistent with expected sea water attenuation (see Figure 4). The overall power spectrum is consistent with that observed during the first 5 hours of data. Also, in low frequency analysis (.0025 Hz to 1 Hz - not shown in plots), frequency peaks corresponding to periods around 70 sec. were again observed.

5. Figure 32 - 9/17/79 and 9/18/79 Data Compilation

This data was recorded with the extended VCO system (with 20 dB pre-amp). The frequency coverage is good to

about 3 Hz where signal strength falls below sensor sensitivity. The seas were relatively calm and the wind was below 10 knots throughout the measurements. The Fredricksburg geomagnetic k indices were 3+ or less during the recording periods (again, geomagnetically quiet). The predominant ocean swell period of about 12.5 seconds (f=.08 Hz) can again be seen. Also, wind driven waves are noted with the spectrum peaks at about .4 Hz. On two of the recordings (curves 1 and 3), peaks around 1 Hz are noted, which correspond to pc1 micropulsations. Again the overall power spectrum level correlates with that observed in the first 9 hours of data.

V. CONCLUSIONS AND SUMMARY

It was originally planned to measure geomagnetic field fluctuations in the .001 Hz to 100 Hz range at a variety of depths, times, and sea conditions on the floor of Monterey Bay. Due to the general smooth nature of the spectrum below .01 Hz, and the length of analysis time involved, the frequency coverage in the analysis was limited to above .01 Hz. The upper end of the frequency coverage was limited to approximately 3 Hz, where the actual field levels approached the limit of the sensor's sensitivity (.005 nT).

Of the fourteen hours of data recorded, only the last four hours cover the entire frequency range (.01 Hz to 3 Hz). One goal of this experiment, to design and manufacture a suitable recording system, was achieved with the extended system used for the last four hours of measurement, within the constraints set by the sensor. The second goal, to obtain geomagnetic fluctuation data on the floor of Monterey Bay, was also achieved, but the quantity of data is quite limited.

Despite the small amount of data, a few general observations can be made. As the spectrum above 3 Hz became level, it was apparent that the background level on the ocean floor was below 2.5×10^{-5} nT^2/Hz at frequencies above 3 Hz. It appears that even relatively close to shore, little, if any, high frequency noise (above 3 Hz) is propagated up through

the ocean's crust into the ocean. In the .05 Hz to 1 Hz range, it appears that ocean wave generated geomagnetic fluctuations dominate the spectrum, their amplitude being directly proportional to the wave height. Although the correlation between ocean wave height and measured geomagnetic fluctuations was limited, the predominant ocean swell (T=10 sec.) was found to produce the correct magnitude of variation as was computed theoretically. This served to give a rough verification of the system's calibration as well as a means of correctly correlating certain peaks in the spectra with surface wave action. There is a possible correlation between the magnetic fluctuation peaks observed around .015 Hz (T=67 sec.) and surface ocean wave grouping at the same frequency. More data is necessary before an exact determination can be made as to whether the peaks are surface wave generated or are caused by pc4 micropulsations.

Attempts were made to project the expected geomagnetic spectrum that would be observed on the surface of the earth through various ocean depths and compare that with observed data. This proved inconclusive since typical variations in expected spectra might vary as much as 10 dB or more in the frequency range of interest, while the attenuation at these shallow depths was of the order of only a few dB. All that can be said is the spectrum levels observed were consistent with those recorded at a land site in Monterey, California in 1978 [Barry 1978]. For more specific conclusions to be drawn, a great quantity of data must be taken at much

greater depths and with concurrent land and sea measurements. From such data it would be possible to determine if any of the geomagnetic fluctuations are being propagated up through the ocean crust.

VI. EQUIPMENT/SYSTEM IMPROVEMENTS AND RECOMMENDATIONS

The final system used for the Monterey Bay measurements (VCO with additional 20 dB pre-amp) has several shortcomings for use in an open ocean environment. The final system expanded the frequency coverage to 3 Hz, where it was limited by sensor sensitivity. Therefore, from a recording system standpoint, further improvements in the system noise is not necessary as it is already below the sensor sensitivity to frequencies well above 3 Hz. The systems final characteristics are listed below:

1. Sensitivity: 5×10^{-3} nT
2. Range: Continuous frequency coverage up to 3 Hz
3. Recording Time: 1 hour
4. Current Drain: Sensor-lamp (30 VDC)
   Recorder- ½ amp (6 VDC)

The DC geomagnetic field data can be retrieved by recording on another channel the output of the first discriminator stage prior to the capacitive coupling in the VCO stage.

Looking at the systems characteristics, it can be seen that two serious problems remain before the system can be used extensively in an open ocean environment:

1. High current usage - The Cesium vapor magnetometer uses 30 VDC power at a 1 amp rate. For extended measurements (i.e. - 1 week), this would take approximately 6 battery packs of the size used for the Monterey Bay

measurements. It would require three spheres to house the batteries required. Additional power for increased recording time is not a problem as the tape length is the limiting factor in recording time.

2. Short recording time - for extended measurements, analog recording is impractical. Reducing recorder speed by one half would give 2 hour recording times and cascading tape recorders could increase the time by 2 hours for each recorder, but for periods of days or weeks, this isn't feasible. The solution is to digitize the signal and then record it. At present work is being done to design and manufacture a digital system. The sensitivity and frequency coverage of the digital system is being designed so that its noise floor is lower than the present system, therefore, sensor sensitivity will still be the limiting factor for frequency coverage. The length of recording time would be governed by the repetition rate of the digital system (this would also dictate the upper frequency limit).

One approach to extended measurements using the present systems would be to use a programmer and several recorders. This could be set up fairly easily so that several one hour samples could be taken spaced over several days.

Another sensor that is being actively investigated is a 6000 turn coil antenna. This could solve the high power requirements problem of the sensor as the only sensor power required is for a pre-amp on the output of the coil.

This could also increase frequency coverage as the sensitivity is proportional to the frequency. The shortcomings of the coil as a sensor is the limited low frequency sensitivity ($\gtrsim$ .1 Hz) and the inability to measure the D.C. geomagnetic field.

Based on the above considerations, the following system is recommended for extended long term measurements in an open ocean environment:

1. Automatic release system so that the entire system can be dropped to the ocean floor and retrieved at some later date. Work is presently underway on a cement block weighted system with a timed explosive release.

2. Sensor - Cs vapor magnetometer with increased battery packs to be turned on and off by a master timing system.

3. Recording Electronics System - identical to the one used in this experiment with the addition of a digitizing system after the VCO stage and prior to the recorder capable of interrogating the output of the VCO (for high sensitivity) and the output of the first discriminator stage (to obtain the total DC geomagnetic field).

4. Master timing system - capable of energizing the sensor and recording system electronics at pre-selected times so that measurements can be extended to cover weeks, even months.

With this system, very sensitive and long term measurements can be made. To increase the sensitivity of

the system, the possibility of using super conducting magnetometers could be considered, however, the frequency coverage gain would be minimal since attenuation above a few Hz is so great at deep depths, the signal strength would still limit coverage to below 10 Hz. It is for this same reason, that the coil as a sensor in a deep ocean environment won't appreciable increase the frequency coverage, and its low frequency limitations make its use unattractive for long term ocean measurements.

The following recommendations are made with repect to the type of follow-on measurements:

1. Ocean wave and concurrent geomagnetic variation data with the wave buoy and geomagnetic sensor in the same physical location so that more direct correlative measurements can be made.

2. Ocean geomagnetic variation recordings with concurrent land geomagnetic recordings in the same general physical area so that correlative analysis can be conducted.

3. Concurrent ocean geomagnetic variation recordings in several locations on the ocean floor, including deep sites, to conduct spatial coherence analysis.

APPENDIX A

EQUIPMENT SCHEMATICS

Figure 34 is the schematic for the VCO unit used in this experiment. The 20 dB pre-amp used for the extended system is also included in Figure 34. Figure 35 is the schematic for the mixer circuit used at output of the analog cassette recorder for data analysis. Also included in Figure 35 is the 2 KHz oscillator used as the reference signal to the analog cassette recorder.

VCO UNIT

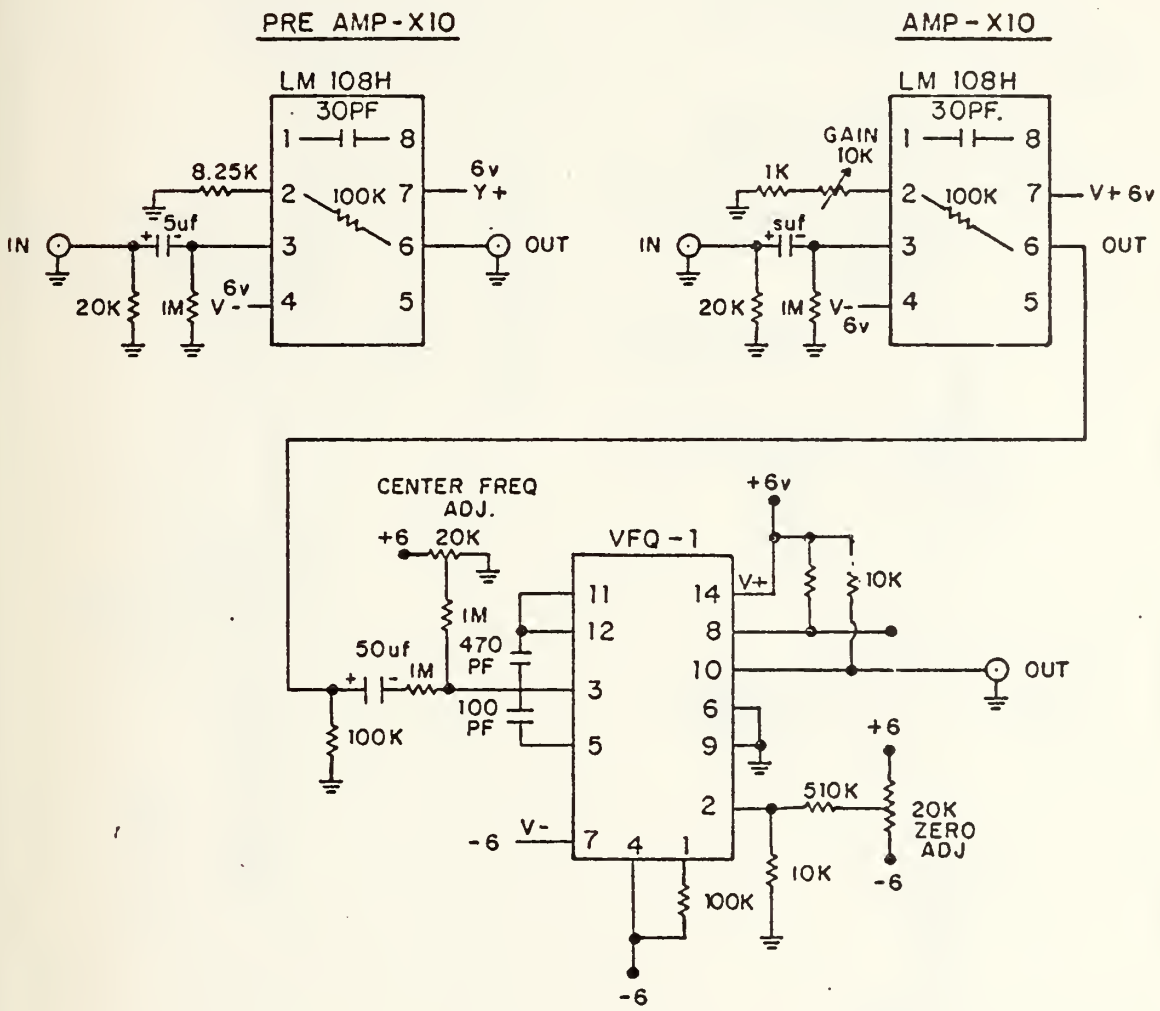

Figure 34.

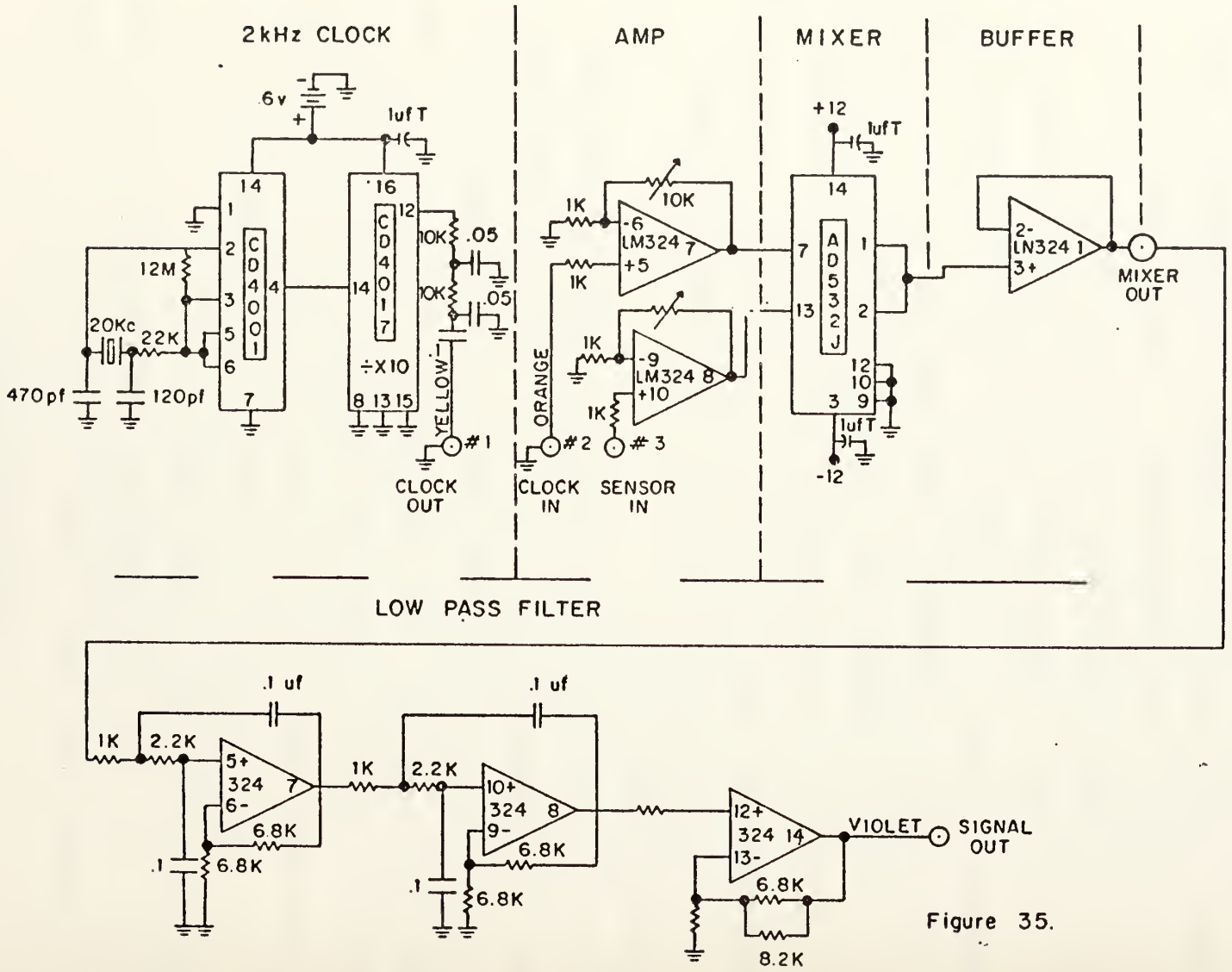
2kHz CLOCK
AMP
MIXER
BUFFER
6v
1uf T
12M
20Kc
22K
470pf
120pf
CD4001
÷X10
10K
.05
YELLOW
#1
CLOCK OUT
1K
10K
LM324
ORANGE
#2
#3
CLOCK IN
SENSOR IN
+12
-12
AD532J
MIXER OUT
LOW PASS FILTER
.1 uf
2.2K
6.8K
VIOLET
SIGNAL OUT
8.2K

Figure 35.

APPENDIX B

SYSTEM USAGE NOTES

Following are some equipment usage notes that might prove helpful for others that might use the geomagnetic data recording system discussed in this thesis.

1. Glass spheres - the surface of the spheres are ground and matched. When mating, ensure serial numbers of the two hemispheres match and that the indexing arrows on the two hemipheres coincide. When cleaning the surface, use toluene, but only in a well ventilated area and with plastic gloves due to its extremely high toxicity. Avoid scratching the ground surface as this will lead to leakage and resultant equipment damage or loss.

2. Analog Cassette Recorder - clean and demagnetize recording heads after each recording. Prolonged usage without cleaning results in noise spikes (recording head dropout), that is very detrimental when attempting to conduct very low frequency (long analyzation times) analysis. A few of these spikes well placed in a one hour recording can completely ruin a data tape. Ensure record levels are set properly prior to sealing up the system in the glass sphere.

3. VCO unit and 20 dB pre-amp. - pre-set the center frequency at 1500 Hz prior to sealing up the system. There is a labeled potentiometer in the VCO unit, "center frequency adjust". The frequency should be adjusted with the input shorted. Use of the 20 dB pre-amp stage is dependent on depth and sea-state considerations. In rough seas and

relatively shallow depths (< 100 meters) the pre-amp stage should not be used as it will overdrive the VCO unit producing a non-usable output. For deep ocean measurements, use of the 20 dB pre-amp stage is recommended because it lowers the noise floor of the system and ocean waves will not overdrive the VCO unit due to attenuation of the geomagnetic variations by sea water.

4. Mixer - There is an amplifier stage for each of the two input channels of the mixer. There are two potentiometers labeled "gain adjust" inside the mixer. With the data channel and the 2 KHz reference channel as inputs to the mixer, adjust the potentionmeters for a 6-10V peak to peak difference signal. Check the output frequency to ensure it is the difference frequency between the two input signals. Due to record level differences, this procedure may have to be conducted each time a new data tape is analyzed.

5. 2 KHz Oscillator - there is a switch internal to the oscillator casing to energize it. Periodically check the internal battery for proper voltage. Check the output for a 2 KHz signal prior to sealing in the glass sphere.

6. Gell Cell Batteries - As all equipment is powered by batteries, their charge status is of paramount importance. The batteries are designed to maintain the quoted ampere-hour rating and fall off rapidly after this is reached, therefore, just checking the voltage will not suffice to ensure proper power will be maintained during the measurements. It is necessary to maintain some sort of a record

of the current usage on each battery. There are presently two amp-hour ratings being used in the system. The recommended charge procedure is listed below:

18 Amp-hour: Charge at a 1 amp rate for approximately 20 hours for full charge. Do not overcharge for more than 24 hours in excess of the amp-hour rating.

2.6 Amp-hour: Charge at a .2 amp rate for approximately 15 hours for full charge. Do not overcharge for more than 24 hours in excess of the amp-hour rating.

7. Connectors/Cable - All connectors are single pin. Underwater coaxial connectors were initially used, but were found to be fragile and resulted in broken connections. To date, there have been no problems with the single pin connectors. After use, the connectors should be cleaned with alcohol to prevent corrosion. The 200 foot coaxial cable, ending in single pin connectors, has the center lead wired to the male connector at each end. The female connectors are wired to the ground shield of the cable. When using the equipment, ensure the cable and connectors are not subjected to stretching or sharp bends to prevent possible breakage or leakage.

8. General - The spheres have been pressure tested to 15,000 psi. To maintain this rating, it is necessary to ensure the sphere mating surfaces are not scratched and are kept clean. The connectors have been pressure tested to 10,000 psi. The locking sleeves on the connectors are there to prevent stress and are not part of the pressure system.

The 200 foot coaxial cable is designed to carry 5000 volts at 4 amps. The external permanent connections have been used in water depths up to 1000 feet. Prior to usage in the open ocean, it is recommended that they be pressure tested to the pressure expected to be encountered.

LIST OF REFERENCES

1. Barry, J.M., Power Spectra of Geomagnetic Fluctuations Between 0.1 and 10 Hz, M.D. Thesis, Naval Postgraduate School, Monterey, 1978.

2. Bloom, A.L., "Optical Pumping", Scientific American, Oct 1960.

3. Campbell, W.H. and Matsushita, S., Physics of Geomagnetic Phenomena, V. 1,2, Academic Press, 1967.

4. Cladis, J.B., Davidson, G.T., and Newkirk, L.L., The Trapped Radiation Handbook, DNA 2542H, 1971.

5. Clark, R.H., Allen, K.R., and Johnson, R.K., Ocean Wave Measurements with an Array of Bottom-mounted Magnetometers, Paper presented to Geophysics Symposium in Monterey, California, 1979.

6. Clayton, F.W., Power Spectra of Geomagnetic Fluctuations Between 0.1 and 40 Hz, M.D. Thesis, Naval Postgraduate School, Monterey, California, 1979.

7. Fraser-Smith A.C., and Buxton, J.L., "Superconducting Magnetometer Measurements of Geomagnetic Activity in the 0.1 to 14 Hz frequency range", Journal of Geophysical Research, V. 80, No. 27, p. 3141-3147, August 1975.

8. Herron, T.J., "An Average Geomagnetic Power Spectrum for Period Range 4.5 to 12,900 Seconds", Journal of Geophysical Research, V. 72, No. 2, p. 759-761, January 1967.

9. Jacobs, J.A., Goemagnetic Micropulsations, p. 179, Springer, New York, 1970.

10. Kraichman, M.B., Handbook of Electromagnetic Propagation in Conducting Media, Naval Material Command, NAVMAT P-2302, 1976.

11. Naval Underwater Systems Center, Newport, Rhode Island, T.R. 5681, ELF Effective Noise Measurements Taken in Connecticut During 1976, by Peter R. Bannister, 1977.

12. Pacific Sierra, Research TR 706, Land to Seafloor Electromagnetic Transmission in the 0.1 to 10.0 Hz Band, by E.C. Field ET AL, August 1977.

13. Schumann, W.O. and König, H., "Uber die Beobachtung von Atmospherics bei geringsten Frequenzen", Naturwiss-enschafften, V. 41, p. 183, 1954.

14. Weaver, J.T., "Magnetic Variations Associated with Ocean Waves and Swell", Journal of Geophysical Research, V. 70, No. 8, p. 1921-1929, April 1965.

15. Wertz, R., and Campbell, W.H., "Integrated Power Spectra of Geomagnetic Field Variations with Periods of .3 to 300 seconds", Journal of Geophysical Research, V. 81, No. 28, p. 5131-5135, 1966.

16. Wynn, M.J. and Trantham, H.W., A Study of the Electric and Magnetic Fields of Ocean Waves, U.S. Navy Mine Defense Laboratory report number 2743, 1968.

INITIAL DISTRIBUTION LIST

		No. Copies
1.	Defense Documentation Center Cameron Station Alexandria, VA 22314	2
2.	Library, Code 0142 Naval Postgraduate School Monterey, CA 93940	2
3.	Department Chairman, Code 61 Department of Physics and Chemistry Naval Postgraduate School Monterey, CA 93940	1
4.	Professor O. Heinz, Code 61Hz Department of Physics and Chemistry Naval Postgraduate School Monterey, CA 93940	2
5.	Professor Paul H. Moose, Code 61Me Department of Physics and Chemistry Naval Postgraduate School Monterey, CA 93940	2
6.	LT E. J. Chaffee 392C Ricketts Rd. Monterey, CA 93940	1
7.	R. Smith, Code 012A Research Administration Naval Postgraduate School Monterey, CA 93940	1
8.	W. Smith, Code 012A Research Administration Naval Postgraduate School Monterey, CA 93940	1
9.	LT Bert Homan SMC 2759 Naval Postgraduate School Monterey, CA 93940	1
10.	LT Gerald McDevitt SCM 1946 Naval Postgraduate School Monterey, CA 93940	1

11. Professor Warren C. Thompson, Code 68Th — 1
Department of Oceanography
Naval Postgraduate School
Monterey, CA 93940

12. Chief of Naval Research
Department of the Navy
800 North Quincy Street
Arlington, Virginia 22217
Code 100C1 — 1
Code 460 — 1
Code 463 — 1
Code 480 — 1

13. Commanding Officer — 1
Office of Naval Research Branch Office
1030 E. Green Street
Pasadena, CA 91106

14. Director — 1
Naval Research Laboratory
Code 2627
Washington, D.C. 20375

15. Office of Research, Development, Test, and Evaluation — 1
Department of the Navy
Code NOP-987J
Washington, D.C. 20350

16. Director — 1
Defense Advanced Research
Projects Agency
1400 Wilson Boulevard
Arlington, Virginia 22209

17. Air Force Office of Scientific Research — 1
Department of the Air Force Directorate of Physics (MPG)
Building 410
Bolling Air Force Base
Washington, D.C. 20332

18. Army Research Office — 1
Department of the Army
Geosciences Division
Box 12211
Research Triangle Park, North Carolina 27709

Thesis
C33864
c.1
Chaffee
186761
Low frequency geo-
magnetic fluctuations
(.01 to 3 Hz) on the
floor of Monterey Bay.